



KERNFORSCHUNGSANLAGE JÜLICH GmbH

Zentralinstitut für Angewandte Mathematik

**Optimization of Reflector-Boosters
for Solar Flat-Collectors**

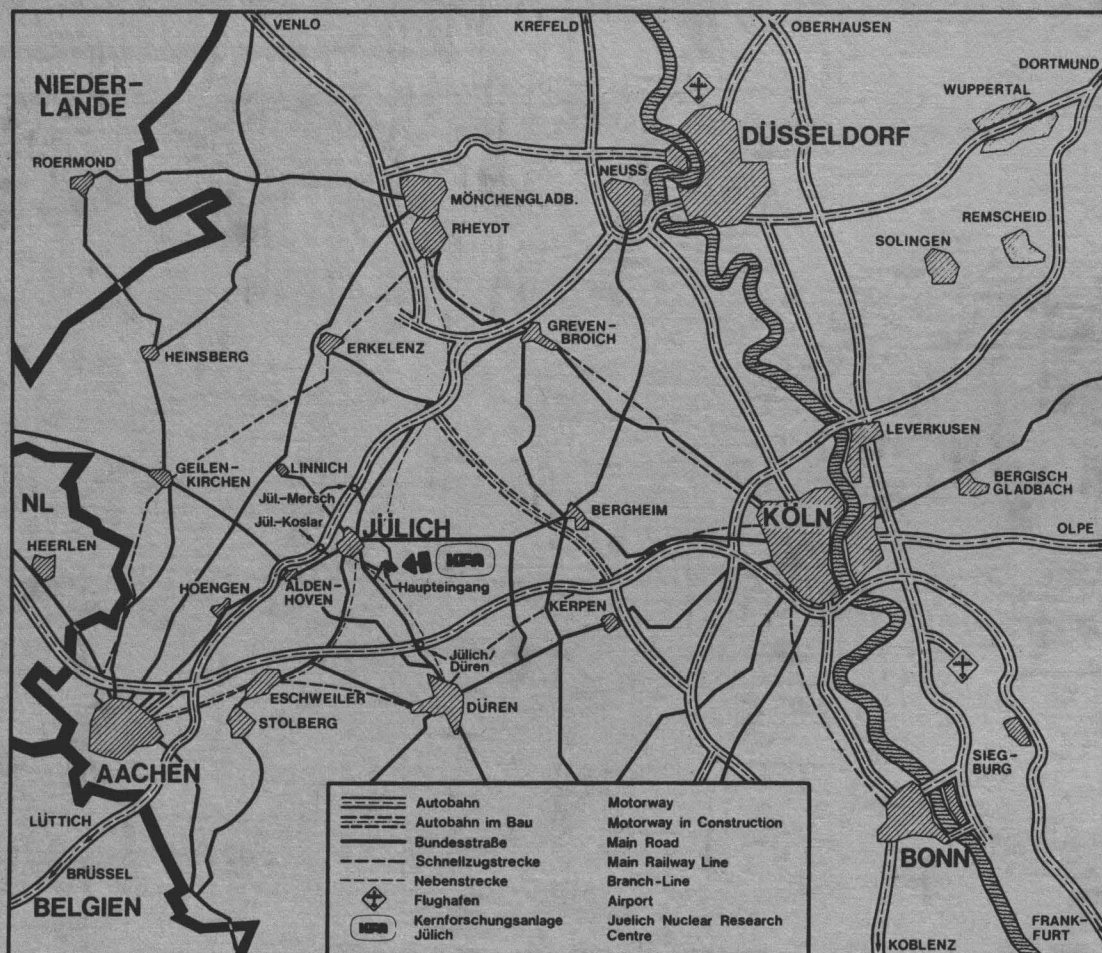
by

M. Profant, P. Weidner, A. Boettcher

Jül - Spez - 37

April 1979

ISSN 0343-7639



Als Manuskript gedruckt

Spezielle Berichte der Kernforschungsanlage Jülich – Nr. 37

Zentralinstitut für Angewandte Mathematik Jül - Spez - 37

Zu beziehen durch: ZENTRALBIBLIOTHEK der Kernforschungsanlage Jülich GmbH,
Jülich, Bundesrepublik Deutschland

Optimization of Reflector-Boosters for Solar Flat-Collectors

by

M. Profant, P. Weidner, A. Boettcher*

***Internationales Büro der KFA Jülich**

The authors would like to express deep appreciation to Dr. Hoßfeld for his fruitful criticism and to M. Liskén, R.D. Kaussen and R. Barluschke for their immense and invaluable programming work.

Abstract:

To increase the working temperature of solar energy systems two-sided collectors together with appropriate reflectors are used. In this paper, we investigate the efficiency of various reflector shapes and try to optimize them under several criteria. The results indicate that with cheap and simply to manufacture reflectors good energy gains can be expected.

Zusammenfassung:

Zweiseitige Kollektoren mit geeigneten Spiegeln können dazu dienen, die Arbeitstemperatur von Solarenergiesystemen zu erhöhen. Wir untersuchen in dieser Arbeit die Wirksamkeit mehrerer Reflektorformen und versuchen, diese unter verschiedenen Kriterien zu optimieren. Die Ergebnisse zeigen, daß billige und leicht zu fertigende Reflektoren gute Leistungsgewinne erwarten lassen.

Introduction

Current efforts to further improve solar collectors have two main goals: Increase of working temperature and decrease of specific cost. Progress in both directions seems possible through adequate use of mirror boosters, which have been proposed years ago (/1/,/2/,/3/).

It was the purpose of this investigation, not only to consider selected cases of using such reflectors as had been done before but to develop a mathematical method which gives the possibility to find optimal reflector forms and positions for all types of solar energy use over the daily and yearly solar cycle.

The paper deals in its first part with the intrinsic possibilities and limitations of "ideal" reflectors, in the second with the efficiency of a reflector as a function of its form and its position with respect to the collector. By parametric studies using the Monte Carlo and subsequently the gradient method, optimal parameter areas can be identified for different solar energy systems.

1. GENERAL CONSIDERATIONS

The purpose of the investigation is to determine a reflector which brings as much additional sun light as possible to the under side of the collector. Nevertheless, for construction reasons some limitations are necessary. As the collector as well as the reflector must be easily accessible for maintenance and cleaning, the distance between collector and ground is approximately 1 meter. Since an installation for gaining solar energy generally will consist of several collectors to be located in not too far distance from each other, the horizontal dimension of the reflector will be limited too. The typical arrangement is shown in Fig. 1.

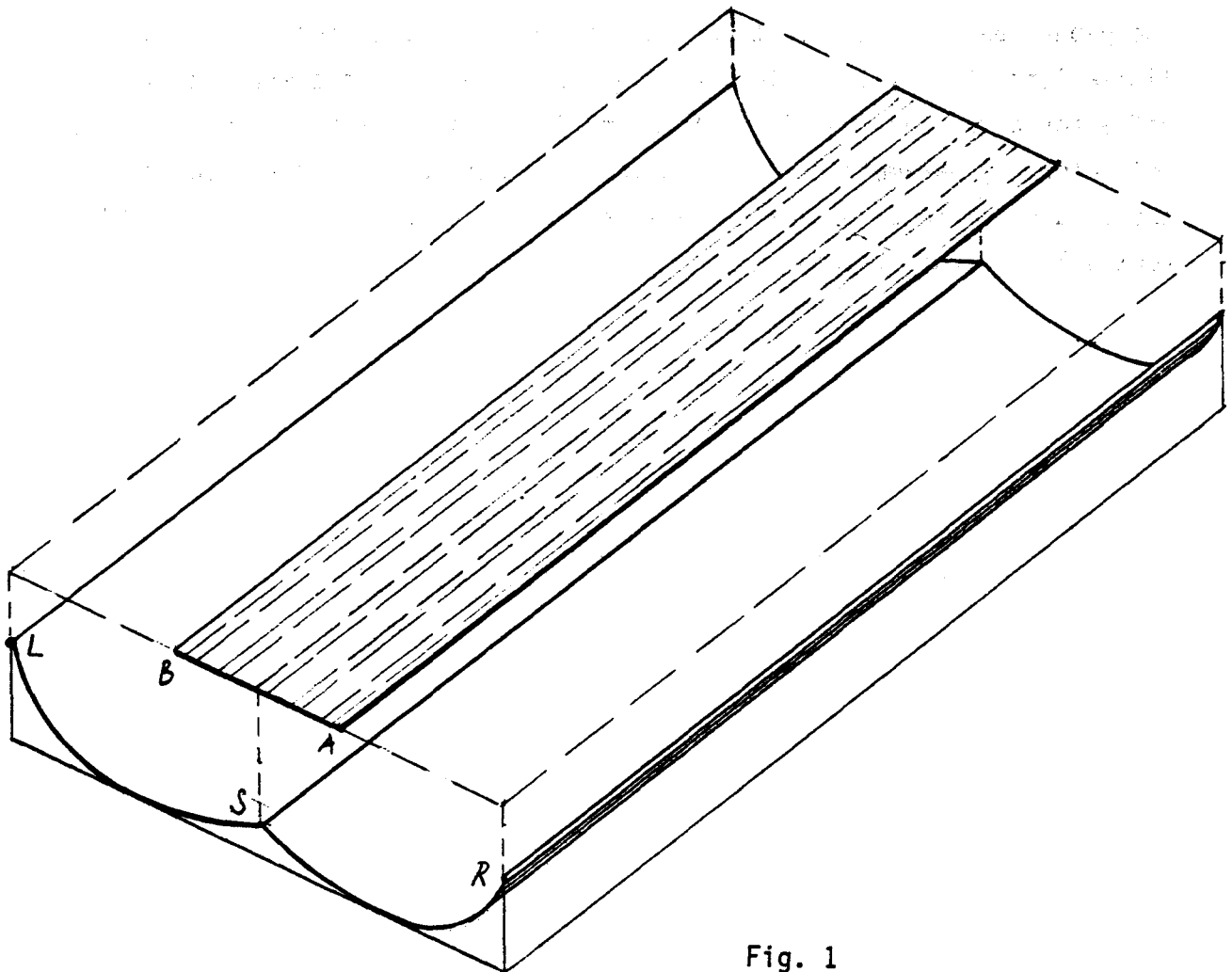


Fig. 1

In order to compare the different reflector shapes it is necessary to find a measure for the quality of a reflector.

To this purpose, we first assume that the longer side of the collector is in north-south direction and that the plane e of the ecliptic is perpendicular to the collector.

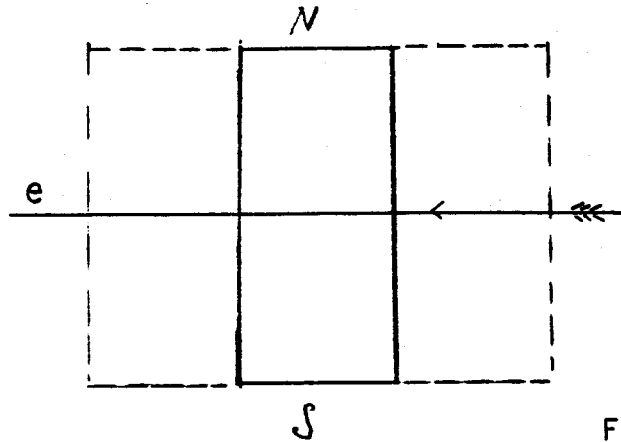


Fig. 2

As is well known, the power of solar radiation on a surface normal to the direction of the radiation is about 1.35 kW/m^2 . This means that the power received at the surface is proportional to the normal cross section of the corresponding ray bundle.

For the arrangement of Fig. 2 the considerations are simplified, because (Fig. 3) the power is only proportional to the width of the ray bundle; the length of the collector (or reflector) affects only the factor of proportionality.

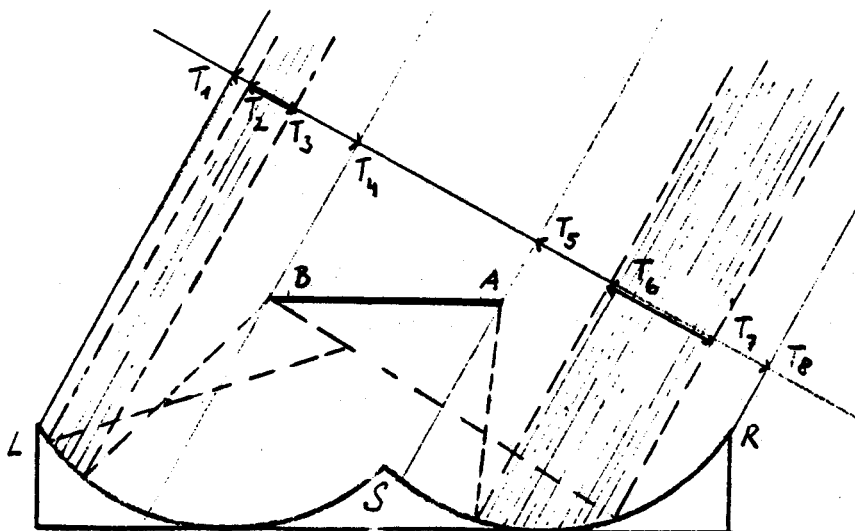


Fig. 3

Therefore, the power on the collector is proportional to the length $\overline{T_4T_5}$ and on the reflector to $\overline{T_1T_4} + \overline{T_5T_8}$. But of the last value only a part is reflected to the under side of the collector. Considering only rays which meet the collector after one reflection (i.e. neglecting multiple reflection), only the portions $\overline{T_2T_3}$ (of $\overline{T_1T_4}$) and $\overline{T_6T_7}$ (of $\overline{T_5T_8}$) hit the collector on the under side. Considering also multiple reflections, the total power would be proportional to $\overline{T_4T_5} + k(\overline{T_2T_3} + \overline{T_6T_7}) + k^2(\dots) + k^3(\dots) + \dots$, k with $0 < k < 1$ being the factor of reflection; here the powers of k higher than one correspond to the multiple reflections. Therefore the calculations which consider only the first reflection give a lower limit for the total power.

Now we return to our original question and define measures for the quality of the reflector.

One reasonable possibility is to choose the ratio of the power I_r , ($I_r \sim \overline{T_2T_3} + \overline{T_6T_7}$), reflected on the collector by the reflector, to the total power I_e ($I_e \sim \overline{T_1T_4} + \overline{T_5T_8}$) falling on the reflector, as "efficiency" γ of the reflector.

The possible values of the quantity $\frac{I_r}{I_e}$ are between 0 and 1; an optimum reflector ($\gamma = 1$) would reflect all incoming sun-rays to the under side of the collector. Another reasonable measure of quality is the quotient of the power reflected by the reflector to the under side of the collector and of the power directly falling on the upper surface of the collector,

$$\gamma' = \frac{I_r}{I_k} \left(= \frac{\overline{T_2T_3} + \overline{T_6T_7}}{\overline{T_4T_5}} \right) ;$$

γ' may assume values larger than 1 for sufficiently large reflectors.

Of course, the quantities γ and γ' depend primarily on the angle of incidence of the sun rays, i.e. on the time of day.

But we carry out our investigations for a fixed reflector, i.e. we will estimate its quality for all angles from a certain range $(\kappa_1, \pi - \kappa_1)$, not only for one angle of incidence.

Let κ be the angle of incidence; then $\gamma = \gamma(\kappa)$ is a function of κ , symmetric with respect to $\kappa = \frac{\pi}{2}$, and the mean

$$\bar{\gamma} = \frac{1}{\frac{\pi}{2} - \kappa_1} \int_{\kappa_1}^{\frac{\pi}{2}} \gamma(\kappa) d\kappa$$

can serve as a measure for the global estimation of the quality. Moreover, we calculate the quantity

$$\bar{\gamma}_1 = \frac{\int_{\kappa_1}^{\frac{\pi}{2}} I_r(\kappa) d\kappa}{\int_{\kappa_1}^{\frac{\pi}{2}} I_k(\kappa) d\kappa} = \frac{\int_{\kappa_1}^{\frac{\pi}{2}} I_r(\kappa) d\kappa}{AB \cdot \cos \kappa_1},$$

and optimize the reflector with respect to $\bar{\gamma}$ or $\bar{\gamma}_1$.

Up to now, we have assumed that the plane e of the ecliptic is normal to the plane of the collector. But this is only an exceptional case, more realistic is the situation of Fig. 4.

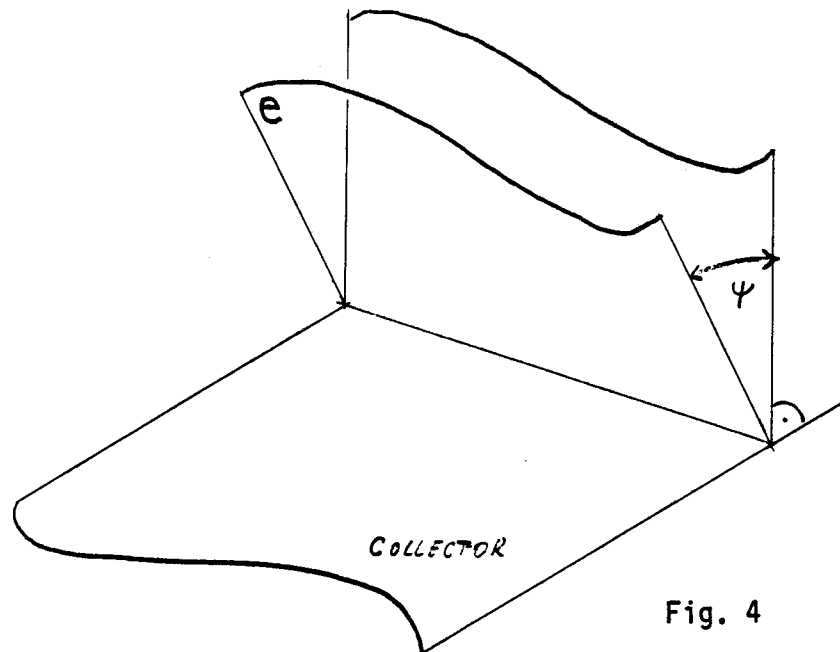


Fig. 4

For the moment we assume a collector of infinite length. In this case (Fig. 5) we see that a ray is reflected to the collector if and only if this is true for its vertical projection. Therefore, we can calculate γ for the vertical projection of the rays as in Fig. 3, and take it as a significant measure for the quality of the reflector. Moreover, we can

prove that this quantity γ (for the projection) is again a quotient of the reflected power I_r to the received power I_e . Whereas I_r and I_e become infinite for a collector of infinite length, their quotient has a finite value.

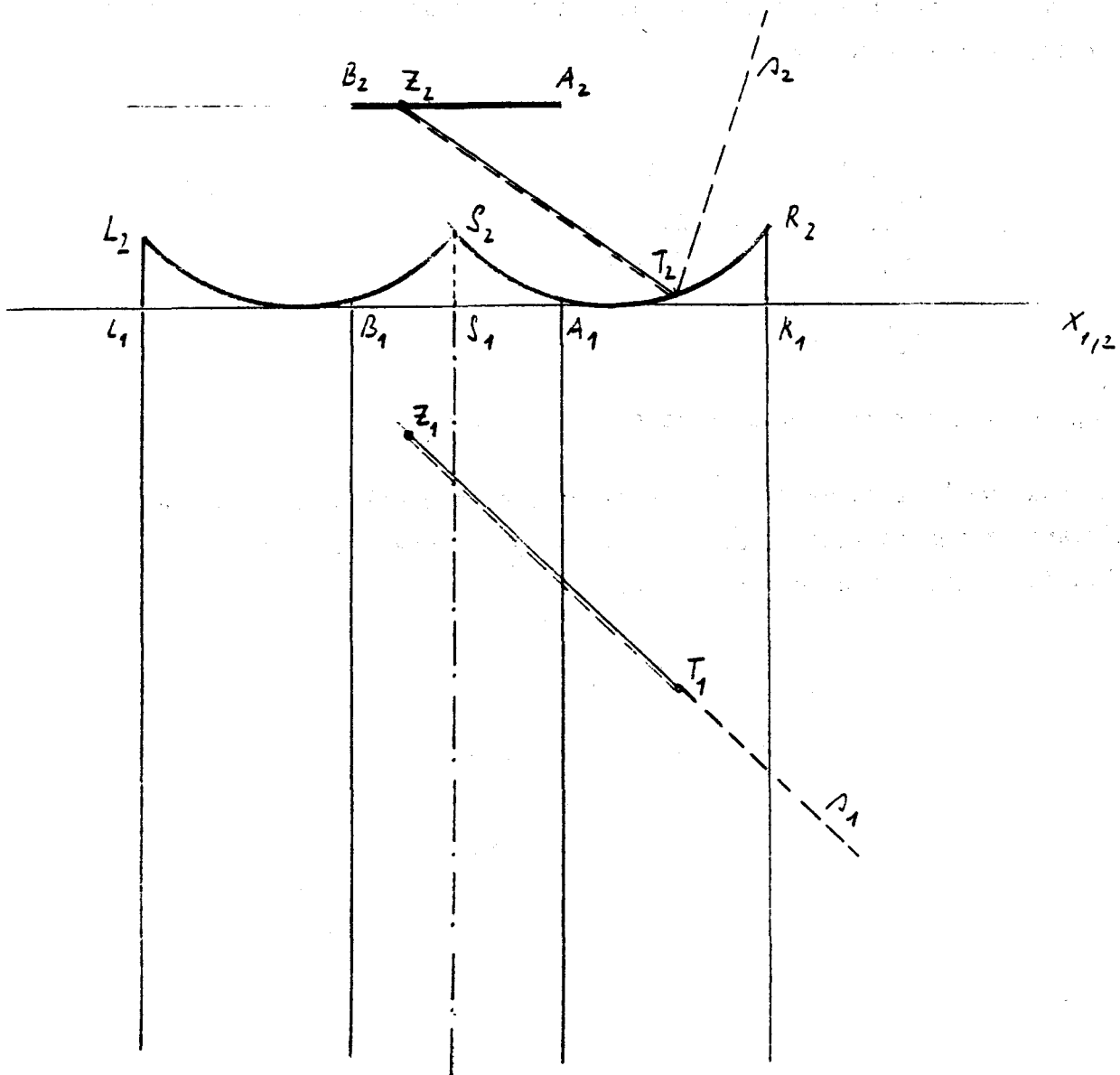


Fig. 5

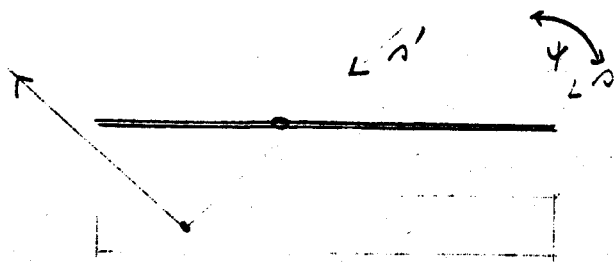


Fig. 6

For a collector of finite length we lose a portion of I_r (Fig. 6) on the ends. Great angles ψ and a short collector cause greater losses.

We summarize our results: For the estimation of the quality of a reflector it suffices to confine oneself to the normal plane of the ecliptic and to calculate γ for this plane. γ represents the useful reflected portion of the power hitting the reflector; this is exact for $\psi = 0$ and approximately for $\psi \neq 0$; the approximation is the better the smaller is ψ and the longer is the collector.

2. THE IDEAL REFLECTOR

In the following we investigate which theoretical limitations exist for the efficiency of a reflector, if the space limitations explained above (height over ground, horizontal distance to next reflector-collector system) are considered as given. We will prove that only rays from a certain range of angles of incidence will be completely reflected on the under side of the collector. The notations are the same as in Fig. 7.

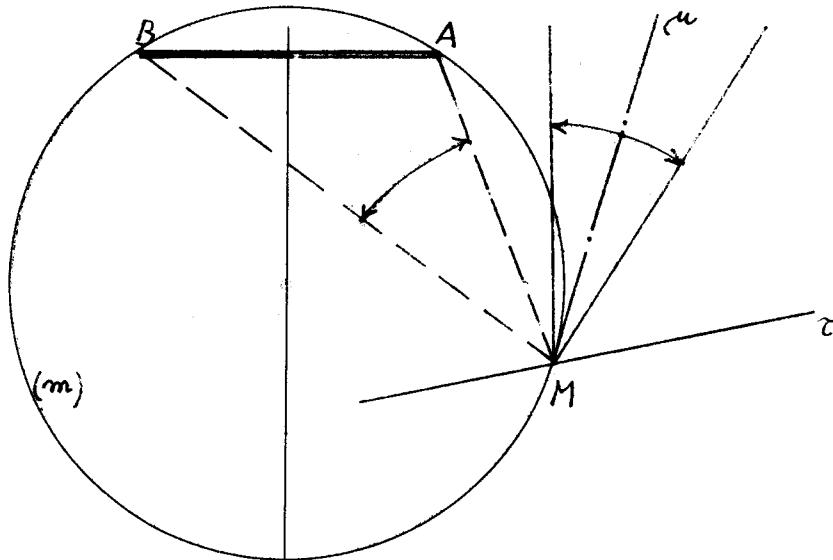


Fig. 7

Looking from any point M of the reflector, the collector will appear under the viewing angle BMA. This means that only rays reflected into this angle will hit the collector. Which of the incident rays these are, depends on two quantities: the angle of incidence μ and the direction τ of the tangent at M to the reflector. If one of these two quantities is chosen, the other one is determined by the requirement that the whole under side of the collector has to be illuminated. From elementary geometry (peripheral angle subtending the chord) we deduce that for all points on a circle (m) the viewing angle and therefore the angle of incidence is of equal size. Considering the space limitations in horizontal direction (Fig.8), the equation

$$\tan \omega_1 = \frac{AB}{2 \sqrt{RB \cdot RA}}$$

for the maximum possible viewing angle ω_1 at the boundary follows from the condition that the above mentioned circle of constant viewing angle is tangent to the lateral borderline. The point of contact is generally located too low (Fig. 8).

Therefore a smaller value ω has to be established, which is determined from (Fig. 9)

$$\tan \omega = \frac{AB \cdot RT}{RT^2 + RB \cdot RA},$$

with the boundary point T of the reflector being fixed.

To choose this point suitably the following table is useful, where for values of \overline{OR} and \overline{OT} the maximum angle ω is noted respectively.

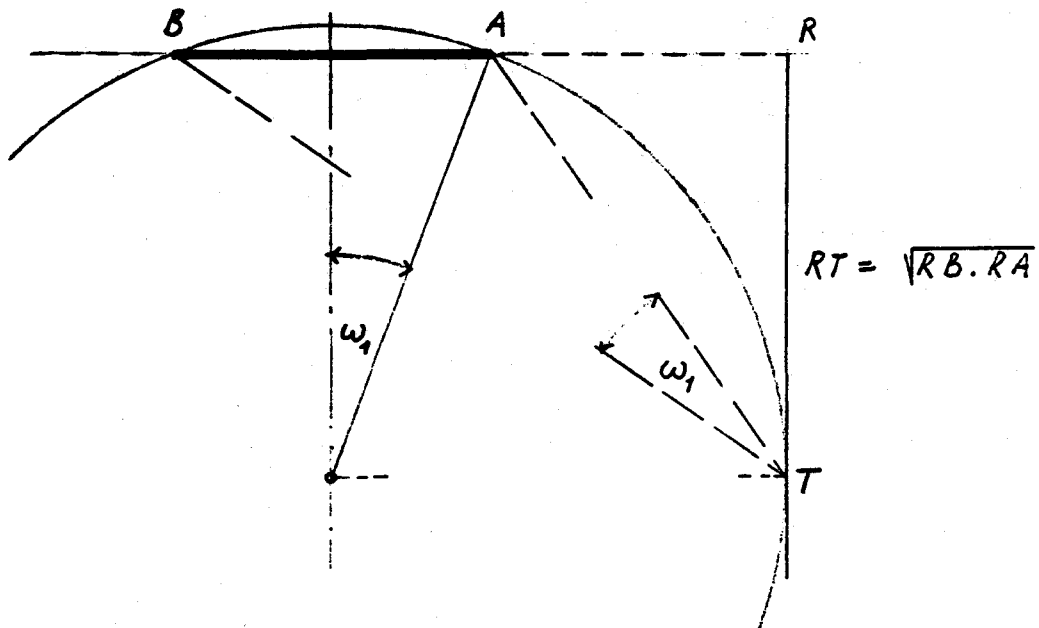


Fig. 8

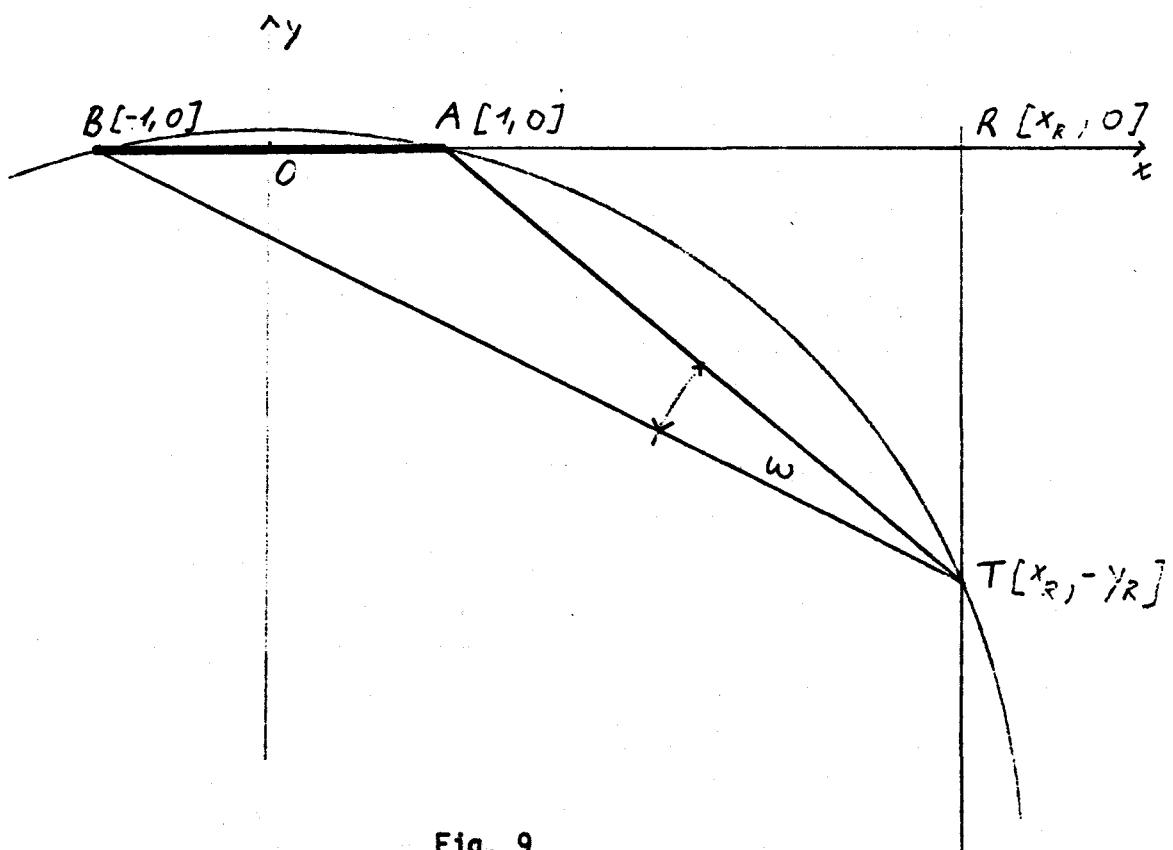


Fig. 9

YR\XR	2.0	2.1	2.2	2.3	2.4	2.5	2.6	2.7	2.8	2.9	3.0	3.1	3.2	3.3	3.4	3.5	3.6	3.7	3.8	3.9
1.0	26.6	24.4	22.5	20.7	19.1	17.7	16.5	15.3	14.3	13.4	12.5	11.8	11.1	10.4	9.8	9.3	8.8	8.3	7.9	7.5
1.1	27.6	25.5	23.5	21.8	20.2	18.8	17.5	16.3	15.3	14.3	13.4	12.6	11.9	11.2	10.6	10.0	9.5	9.0	8.5	8.1
1.2	28.4	26.3	24.4	22.7	21.2	19.7	18.4	17.2	16.2	15.2	14.3	13.4	12.7	12.0	11.3	10.7	10.2	9.6	9.2	8.7
1.3	29.0	27.0	25.2	23.5	22.0	20.5	19.2	18.0	17.0	15.9	15.0	14.2	13.4	12.7	12.0	11.4	10.8	10.2	9.8	9.3
1.4	29.4	27.5	25.8	24.1	22.6	21.2	19.9	18.7	17.7	16.6	15.7	14.8	14.0	13.3	12.6	12.0	11.4	10.8	10.3	9.8
1.5	29.7	27.9	26.2	24.6	23.2	21.8	20.5	19.4	18.3	17.3	16.3	15.4	14.6	13.9	13.2	12.5	11.9	11.4	10.8	10.3
1.6	29.9	28.2	26.6	25.0	23.6	22.3	21.0	19.9	18.8	17.8	16.9	16.0	15.2	14.4	13.7	13.0	12.4	11.9	11.3	10.8
1.7	30.0	28.4	26.8	25.3	24.0	22.7	21.5	20.3	19.3	18.3	17.3	16.5	15.7	14.9	14.2	13.5	12.9	12.3	11.8	11.2
1.8	30.0	28.4	27.0	25.6	24.2	23.0	21.8	20.7	19.7	18.7	17.8	16.9	16.1	15.3	14.6	14.0	13.3	12.7	12.2	11.7
1.9	29.9	28.4	27.0	25.7	24.4	23.2	22.1	21.0	20.0	19.0	18.1	17.3	16.5	15.7	15.0	14.3	13.7	13.1	12.6	12.0
2.0	29.7	28.4	27.0	25.8	24.5	23.4	22.3	21.2	20.3	19.3	18.4	17.6	16.8	16.1	15.4	14.7	14.1	13.5	12.9	12.4
2.1	29.5	28.2	27.0	25.8	24.6	23.5	22.4	21.4	20.5	19.6	18.7	17.9	17.1	16.4	15.7	15.0	14.4	13.8	13.2	12.7
2.2	29.3	28.1	26.9	25.7	24.6	23.6	22.5	21.6	20.6	19.8	18.9	18.1	17.4	16.6	15.9	15.3	14.7	14.1	13.5	13.0
2.3	29.0	27.9	26.7	25.6	24.6	23.6	22.6	21.7	20.8	19.9	19.1	18.3	17.6	16.9	16.2	15.5	14.9	14.4	13.8	13.3
2.4	28.7	27.6	26.6	25.5	24.5	23.6	22.6	21.7	20.9	20.0	19.2	18.5	17.7	17.1	16.4	15.8	15.2	14.6	14.0	13.5
2.5	28.4	27.4	26.4	25.4	24.4	23.5	22.6	21.7	20.9	20.1	19.3	18.6	17.9	17.2	16.6	15.9	15.4	14.8	14.2	13.7
2.6	28.0	27.1	26.1	25.2	24.3	23.4	22.6	21.7	20.9	20.2	19.4	18.7	18.0	17.3	16.7	16.1	15.5	15.0	14.4	13.9
2.7	27.7	26.8	25.9	25.0	24.1	23.3	22.5	21.7	20.9	20.2	19.5	18.8	18.1	17.4	16.8	16.2	15.7	15.1	14.6	14.1
2.8	27.3	26.5	25.6	24.8	24.0	23.2	22.4	21.6	20.9	20.2	19.5	18.8	18.2	17.5	16.9	16.3	15.8	15.3	14.7	14.3
2.9	26.9	26.1	25.3	24.5	23.8	23.0	22.3	21.5	20.8	20.1	19.5	18.8	18.2	17.6	17.0	16.4	15.9	15.4	14.9	14.4
3.0	26.6	25.8	25.0	24.3	23.6	22.8	22.1	21.4	20.7	20.1	19.4	18.8	18.2	17.6	17.1	16.5	16.0	15.5	15.0	14.5
3.1	26.2	25.5	24.7	24.0	23.3	22.6	22.0	21.3	20.7	20.0	19.4	18.8	18.2	17.6	17.1	16.6	16.0	15.5	15.1	14.6
3.2	25.8	25.1	24.4	23.8	23.1	22.4	21.8	21.2	20.5	19.9	19.3	18.8	18.2	17.6	17.1	16.6	16.1	15.6	15.1	14.7
3.3	25.4	24.8	24.1	23.5	22.9	22.2	21.6	21.0	20.4	19.8	19.3	18.7	18.2	17.6	17.1	16.6	16.1	15.6	15.2	14.7
3.4	25.0	24.4	23.8	23.2	22.6	22.0	21.4	20.9	20.3	19.7	19.2	18.6	18.1	17.6	17.1	16.6	16.1	15.7	15.2	14.8
3.5	24.7	24.1	23.5	22.9	22.4	21.8	21.2	20.7	20.1	19.6	19.1	18.6	18.0	17.5	17.1	16.6	16.1	15.7	15.2	14.8
3.6	24.3	23.7	23.2	22.7	22.1	21.6	21.0	20.5	20.0	19.5	19.0	18.5	18.0	17.5	17.0	16.6	16.1	15.7	15.3	14.8
3.7	23.9	23.4	22.9	22.4	21.9	21.3	20.8	20.3	19.8	19.3	18.8	18.4	17.9	17.4	17.0	16.5	16.1	15.7	15.3	14.9
3.8	23.5	23.1	22.6	22.1	21.6	21.1	20.6	20.1	19.7	19.2	18.7	18.2	17.8	17.3	16.9	16.5	16.1	15.6	15.2	14.9
3.9	23.2	22.7	22.3	21.8	21.3	20.9	20.4	19.9	19.5	19.0	18.6	18.1	17.7	17.3	16.8	16.4	16.0	15.6	15.2	14.8
4.0	22.8	22.4	22.0	21.5	21.1	20.6	20.2	19.7	19.3	18.9	18.4	18.0	17.6	17.2	16.8	16.4	16.0	15.6	15.2	14.8

The maximum ω for the reflector with the boundary point as in Fig. 9

As has been stated above, the direction of the tangent τ depends on the angle μ . μ now is kept constant and τ is determined for every point by the requirement that the complete collector has to be illuminated from below. As τ is the slope of the tangent at a point of the reflector, we get a differential equation for the shape of the reflector. Some lengthy but elementary calculations will yield

$$y' = \frac{A \tan \frac{\mu}{2} - 1}{A + \tan \frac{\mu}{2}},$$

$$A = s + \sqrt{1+s^2} + \sqrt{1+(s + \sqrt{1+s^2})^2}, \quad s = \frac{y^2 - x^2 + 1}{2xy}$$

Together with the fixed boundary point T, this is an initial value problem which can be integrated numerically.

The calculation for the whole x-range is not reasonable since, beginning at a certain point (depending on μ), the collector shadows the reflector, i.e. not all rays which could be reflected to the under side of the collector will hit the reflector.

This boundary point G (Fig. 10) is determined by the condition

$$\omega = \pi - \mu - \frac{\alpha - \beta}{2}.$$

As also $\omega = \alpha$ is valid, it follows: $2\pi - 2\mu + \beta = 3\alpha$.

For the coordinates x and y of this point the equations holds:

$$\begin{aligned} y \left[(x^2 + y^2 - 1) \sin 2\mu - 2y \cos 2\mu \right] = \\ = (x-1) \left[\sqrt{(x-1)^2 + y^2} \sqrt{(x+1)^2 + y^2} + (1 - x^2 - y^2) \cos 2\mu - 2y \sin 2\mu \right] \end{aligned}$$

During the numerical integration, it is permanently tested whether this equation already is fulfilled. For $\mu = \frac{\pi}{2}$ the equation is simplified to

$$y = -|x-1| \sqrt{\frac{2-x}{2+x}}.$$

The following consideration yields an angular range as large as possible to be reflected on the under side of the collector.

Retaining the mean angle of incidence μ constant, only part of the under side of the collector would be hit by the sun-rays. Therefore it is permitted that the mean angle of incidence is not always the same for all points of the reflector beyond the boundary point. If the requirement is retained that the under side is completely covered by the rays and that the mean angle of incidence differs only as little as possible from μ , we get an actual range of incidence by reflecting the reflected range of angle in the line between the right end of the collector and the reflector point considered (Fig. 10). This line must be perpendicular to the reflector at every point. This implies that the reflector must consist of a circular arc beginning at the boundary point, the centre of which has to be the right hand end of the collector. The circle has the radius

$$\rho = \sqrt{(x_G - 1)^2 + y_G^2}.$$

The next figures show solutions of the differential equation with the subsequent circular arcs for different values of μ and different reflector boundary points.

With respect to the "optimum" reflector the results up till now are only limiting values for practice. For usefulness it is much more important to investigate the efficiency γ or γ' as a function of the angle of incidence according to the above mentioned definition. For this purpose at first the limits of the angle range reflected upon the lower side of the collector have to be determined for every point (x, y) of the reflector.

These limiting angles are denoted by $\Gamma_1(x)$ and $\Gamma_2(x)$.

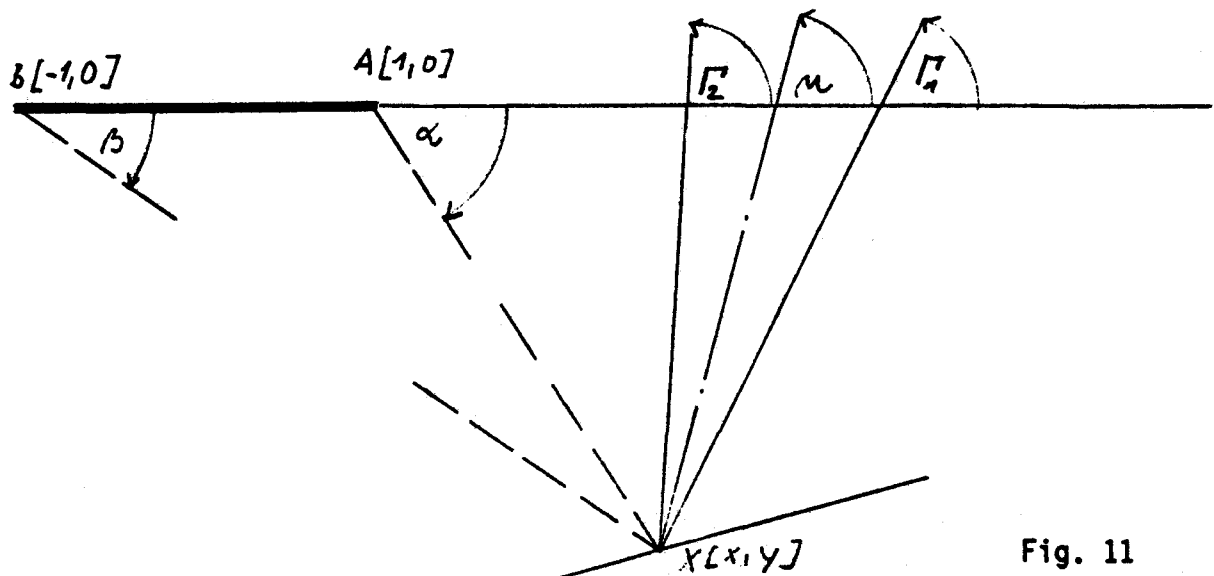


Fig. 11

In the circular part of the reflector, $\Gamma_1(x) = \pi + \beta - 2\alpha$ holds with

$$\tan \alpha = \frac{-y}{x-1}, \quad \tan \beta = \frac{-y}{x+1};$$

x and y satisfy the equation for the corresponding circle.

After insertion we get the following equation

$$\Gamma_1 = \max \left\{ \arctan \frac{2y(x^2-1)-y[(x-1)^2-y^2]}{(x+1)[(x-1)^2-y^2]+2y^2(x-1)}, \arctan \frac{y_R-y}{x_R-x}, 0 \right\}.$$

For Γ_2 , simply, $\Gamma_2(x) = \pi - \alpha$ is obtained. For the part of the reflector having the shape of the above determined curve, we obtain

$$\Gamma_1 = \mu - \frac{\alpha - \beta}{2}, \quad \Gamma_2 = \mu + \frac{\alpha - \beta}{2},$$

and expressed in x, y :

$$\begin{aligned} \tan(\mu \pm \frac{\alpha - \beta}{2}) = \\ = \frac{\sqrt{(x-1)^2+y^2} \sqrt{(x+1)^2+y^2} + (1-x^2-y^2) \cos 2\mu \mp 2y \sin 2\mu}{(x^2+y^2-1) \sin 2\mu \mp 2y \cos 2\mu} \end{aligned}$$

In this way Γ_1 and Γ_2 are determined for every point (x, y) of the reflector. To simplify the further considerations, a function $\kappa(x)$ is defined instead of the two functions, Γ_1 and Γ_2 as follows:

The curve of the reflector will be covered twice; at first from S to R then from R to G (Fig. 10). This total procedure will be parametrized by the parameter x , and $\kappa(x)$ will be defined by:

a) $\kappa(x) = \Gamma_1(x)$, when x passes through the range from S to R
(in this direction)

b) in $x = R$, κ jumps from $\Gamma_1(R)$ to $\Gamma_2(R)$

c) $\kappa(x) = \Gamma_2(x)$, when x passes through the range from R to G .

$\kappa(x)$ is a monoton increasing function of x . The value of $\kappa(x)$ at the point of discontinuity can be chosen freely.

The flux I_r , reflected by the reflector onto the collector, may now be determined as a function of κ . I_r is proportional to the width ϵ of the ray bundle, reflected by the reflector to the under side of the collector. For the case $\kappa = \Gamma_1$ and $\kappa = \Gamma_2$ respectively, one finds

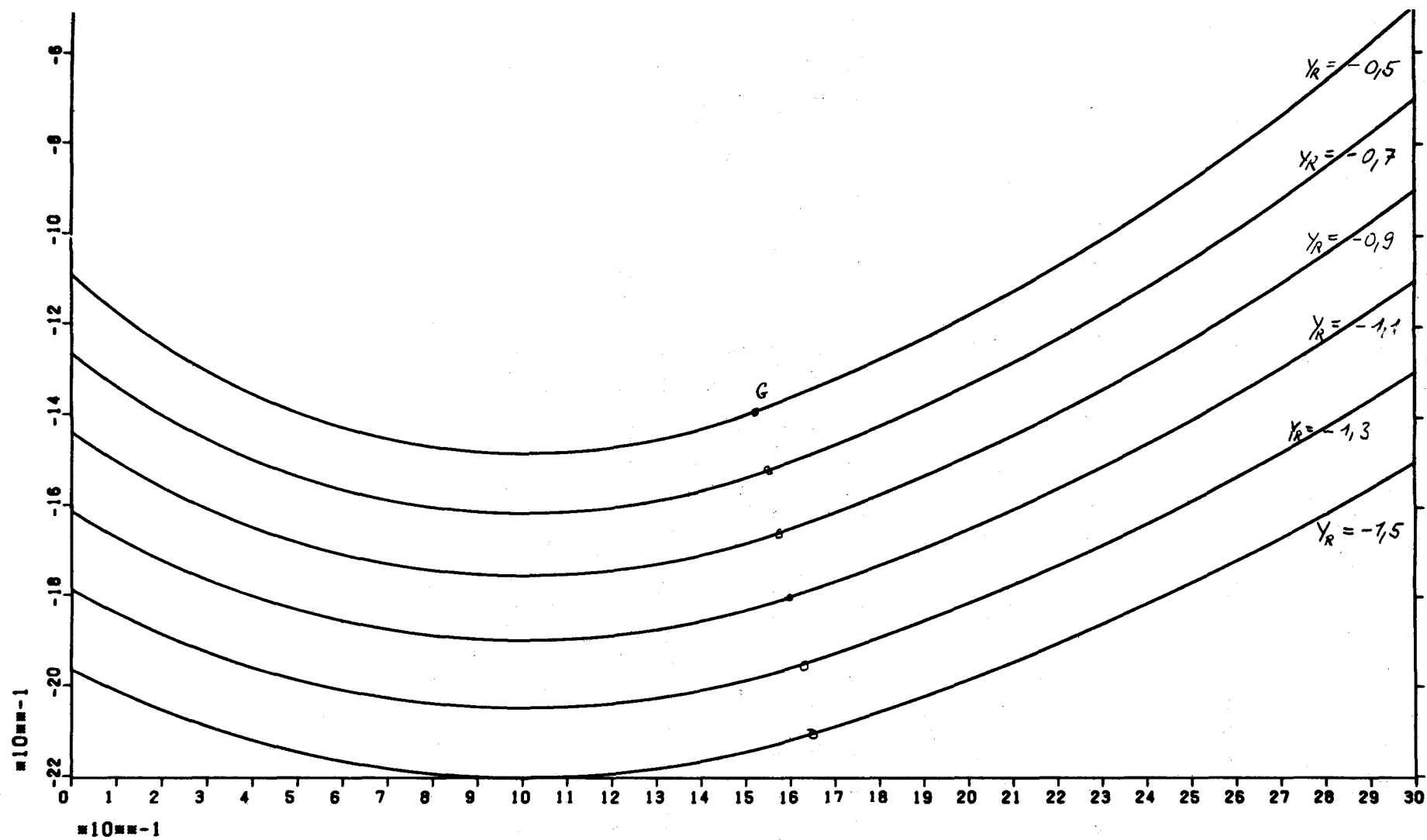
$$\epsilon(\kappa) = \min \left\{ |y \cos \kappa - x \sin \kappa - y_S \cos \kappa|, |y \cos \kappa - x \sin \kappa + \sin \kappa| \right\}.$$

In the case $\Gamma_1(R) \leq \kappa \leq \Gamma_2(R)$, i.e. at the point of discontinuity of κ , one obtains

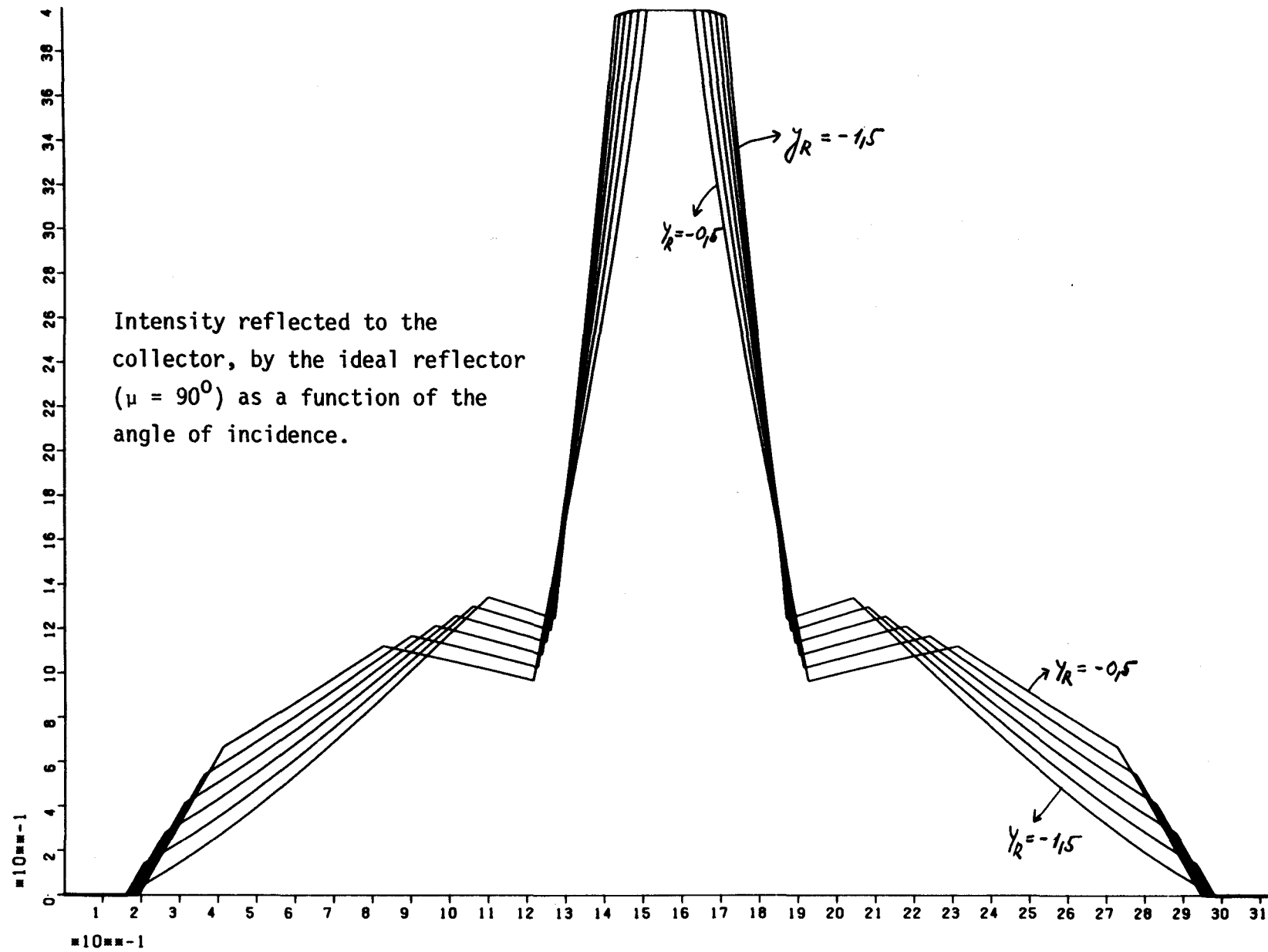
$$\epsilon(\kappa) = \min \left\{ |y_R \cos \kappa - x_R \sin \kappa - y_S \cos \kappa|, |y_R \cos \kappa - x_R \sin \kappa + \sin \kappa| \right\};$$

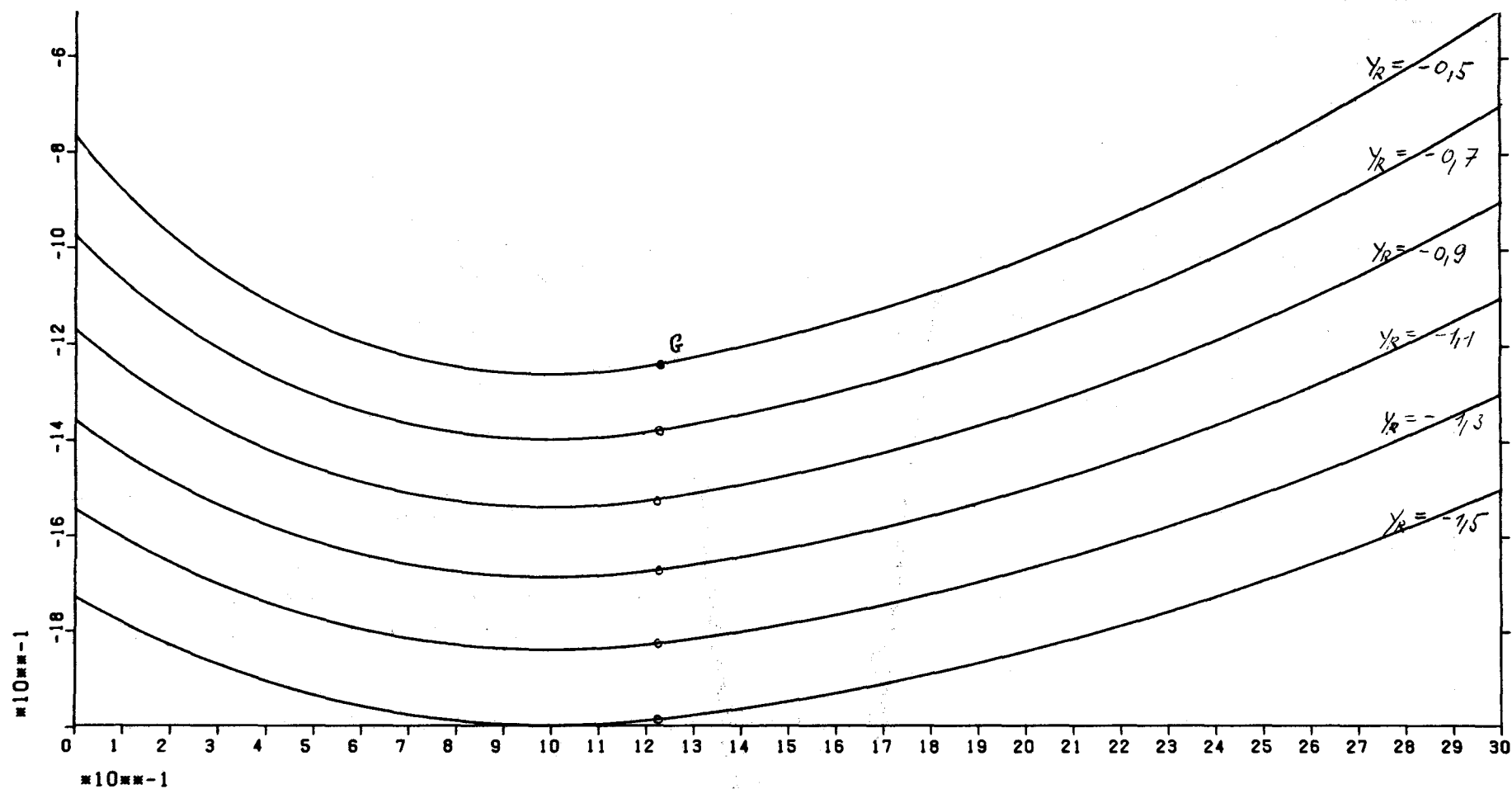
κ can be chosen freely in this case.

The illustrations on pages 15 and 17 display the shape of the ideal reflector for $\mu = 90^\circ$ and $\mu = 75^\circ$, $x_R = 3$ and various values of y_R . If we keep the distance ground-to-collector approximately equal to the length of the collector ($= 2$), we have to choose the boundary-point $x_R = 3$, $y_R = -1.3$ for $\mu = 90^\circ$, and $x_R = 3$, $y_R = -1.5$ for $\mu = 75^\circ$. Accordingly, we extract from the table on page 9 the possible angle range, e.g. $\omega = 15^\circ$ ($= 0.26$ rad) for $x_R = 3$, $y_R = -1.3$; this means that the reflector with the boundary point $x_R = 3$, $y_R = -1.3$ reflects all rays from the range between 82.5° and 97.5° to the collector. However, in this case the reflected flux as a function of the angle of incidence decreases rapidly, as the illustrations on page 16 show. The curve on page 16 also depicts that for the range about $\omega = 23.5^\circ$ ($= 0.41$ rad) the intensity decreases from 4 to 2.8.

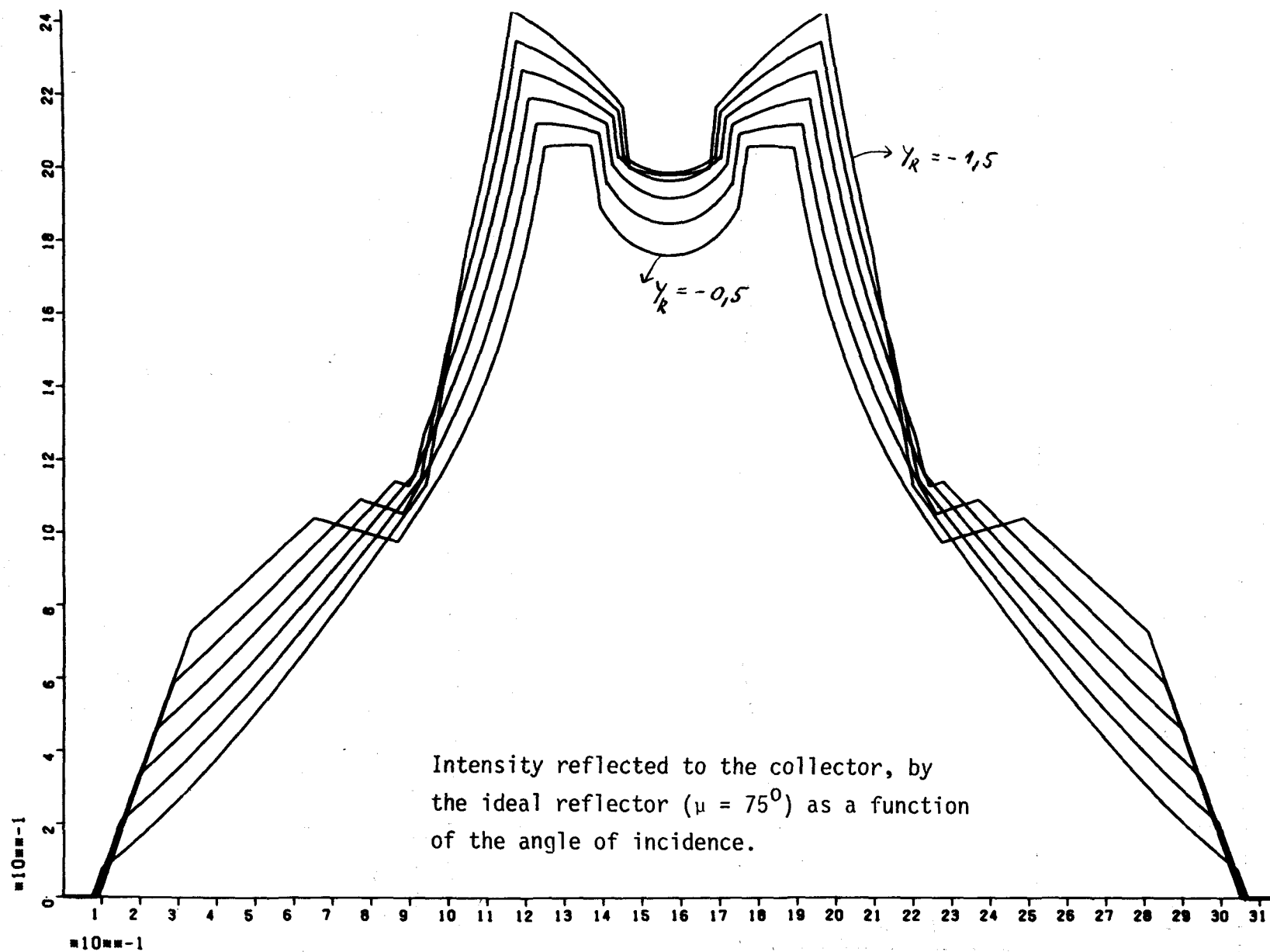


Shape of the ideal reflector for $\mu = 90^\circ$ and various boundary points $(x_R, -y_R)$



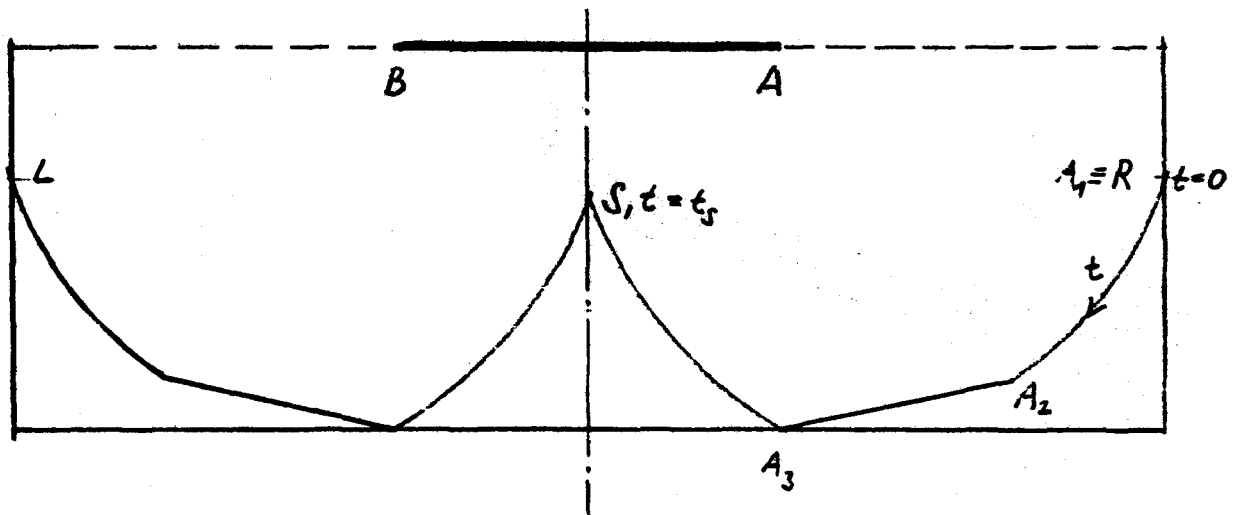


Shape of the ideal reflector for $\mu = 75^\circ$ and various boundary points $(x_R, -y_R)$



3. APPROXIMATE SOLUTION

Now we choose a different point of view. We begin with a known reflector and determine the efficiency for a given angle of incidence κ . For the reflector some limitations are set: it consists of two convex parts symmetrical to each other, each consisting of line segments and circular arcs.



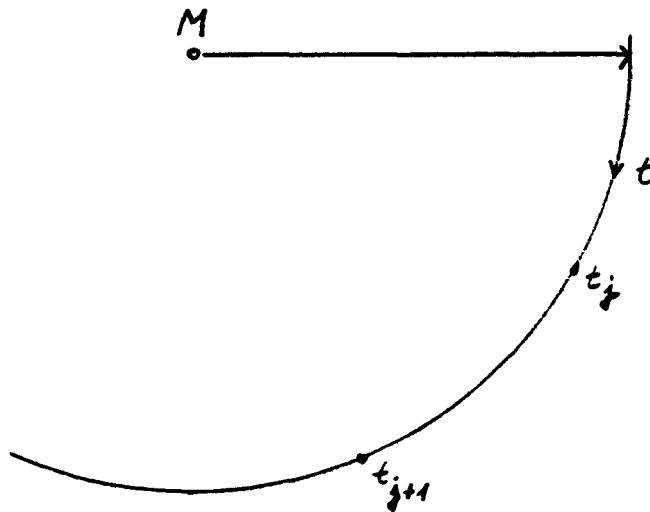
3.1 Description of the reflector

For a reasonable representation of the reflector curve a parameter t is chosen which for both parts passes from 0 to t_s , respectively. The curve is described by $x_R = x_R(t)$ for the right hand part and $x_L = x_L(t)$ for the left hand part. A line segment between the points A_i and A_{i+1} is described by $x = A_i + (t - t_i)(A_{i+1} - A_i)$, the parameter t passing from $t = t_i$ to $t = t_{i+1}$



The data determining this line segment uniquely, are written as a vector with 7 components $(A_i, A_{i+1}, t_i, t_{i+1}, 1)$. The last component 1 is designating a line segment.

A circle segment with centre M and radius r is described by $x = M + r[\cos(t+\tau), -\sin(t+\tau)]$, t passing again from t_j to t_{j+1} with the limitation $t_{j+1} - t_j < \pi/2$. If the piece is longer, it will be represented by two pieces.



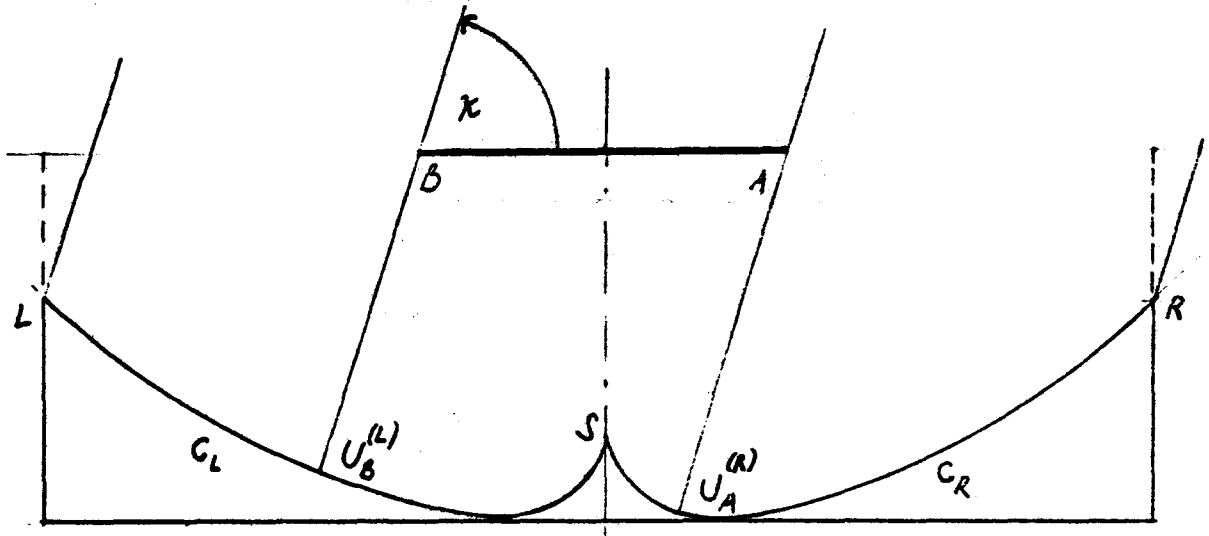
The parameters necessary for the description are again written as a vector: $(M, r, \tau, t_j, t_{j+1}, 0)$. The seventh component 0 shows that we treat a circular arc.

The entire left-hand and right-hand parts of the reflector, respectively, are described by as many vectors as there are line and circle segments. For both halves of the reflector these vectors are combined to matrices D_R and D_L , e.g.

$$D_R = \begin{pmatrix} \overbrace{a_1, a_2}^{A_1} & \overbrace{b_1, b_2}^{A_2} & t_1 & t_2 & 1 \\ \underbrace{m_1, m_2}_M & r, \tau & t_2 & t_3 & 0 \\ \dots\dots\dots \end{pmatrix}$$

The shape of the reflector is completely described by the matrices D_R and D_L . Proceeding from this, for given angles of incidence $\kappa (0 \leq \kappa \leq \frac{\pi}{2})$, the ranges of the reflector can be described which are illuminated and which are shadowed, respectively.

3.2 Illumination of Reflector



From the sketch, it can be seen that the following intersections have to be determined:

$U_R^{(L)}, U_R^{(R)}$: Line through R with C_R and C_L

$U_S^{(L)}$: " " S " C_L

$U_A^{(L)}, U_A^{(R)}$: " " A " C_R and C_L

$U_B^{(L)}$: " " B " C_L

If Z is one of the points R, S, A, B, the line through Z may be written with the parameter s as $Z + s[\cos \kappa, \sin \kappa]$. The intersection of this line with C_R or C_L has now to be determined as an intersection with one of the straight or curved pieces the reflector consists of. If this piece is a line segment, the intersection \bar{t} or \bar{x} , respectively, is obtained by equating $Z + s[\cos \kappa, \sin \kappa]$ and $\underbrace{A_i}_{(a_1, a_2)} + (t - t_i) \cdot \underbrace{(A_{i+1} - A_i)}_{(b_1, b_2)}$.

For $|K| \geq \epsilon$ with $K = (b_1 - a_1) \sin \kappa - (b_2 - a_2) \cos \kappa$ one obtains

$$\bar{t} = t_i + 1/K [(a_2 - z_2) \cos \kappa - (a_1 - z_1) \sin \kappa] \text{ and } \bar{x} = A_i + (\bar{t} - t_i)(A_{i+1} - A_i);$$

ϵ is a small positive number to be suitably chosen. \bar{t} is limited to $t_i \leq \bar{t} \leq t_{i+1}$. For $|K| < \epsilon$ both straight lines have to be considered as parallel, i.e. there is no intersection point.

If the considered part of the reflector is the arc of a circle, then

$$Z+s [\cos \kappa, \sin \kappa] \quad \text{and} \quad M+r [\cos(t+\tau), -\sin(t+\tau)]$$

must intersect. One obtains

$$\sin(\bar{t}+\tau+\kappa) = 1/r [(m_2-z_2)\cos \kappa - (m_1-z_1)\sin \kappa] = \mathcal{A}.$$

For $|\mathcal{A}| \geq 1$ there is no intersection. For $0 < \mathcal{A} < 1$ the following values are obtained

$$\bar{t}_1 = \arcsin \mathcal{A} - \tau - \kappa \quad \text{and} \quad \bar{t}_2 = \pi - \arcsin \mathcal{A} - \tau - \kappa;$$

For $-1 < \mathcal{A} < 0$ we obtain

$$\bar{t}_1 = 2\pi - \tau - \kappa + \arcsin \mathcal{A} \quad \text{and} \quad \bar{t}_2 = \pi - \tau - \kappa - \arcsin \mathcal{A}.$$

If both values \bar{t}_1 and \bar{t}_2 are between t_i and t_{i+1} , then $\bar{t} = \max(\bar{t}_1, \bar{t}_2)$ has to be chosen. The intersection then is: $\bar{x} = M+r [\cos(\bar{t}+\tau), -\sin(\bar{t}+\tau)]$.

If all existing intersections are determined in this way, it has to be decided which part of the reflector is illuminated and which is shadowed. For this purpose a straight line is directed through the centre of the collector (origin) perpendicular to the direction of incidence of the rays.

A normal vector to this straight line is $(\sin \kappa, -\cos \kappa)$, if κ is the angle of incidence of the rays. The projection of the "boundary points" A, B, S, L, R on this straight line gives the points P_A, P_B, P_S, P_L, P_R . The coordinates of these points on the straight line are called T_A, T_B, T_S, T_L, T_R . For T_R , for instance, one obtains (as scalar product) $a_R \sin \kappa - b_R \cos \kappa$, where (a_R, b_R) are the coordinates of R. If the larger of the values T_A and T_L is called T_M , three cases may be discerned:

$$1) T_S \leq T_M$$

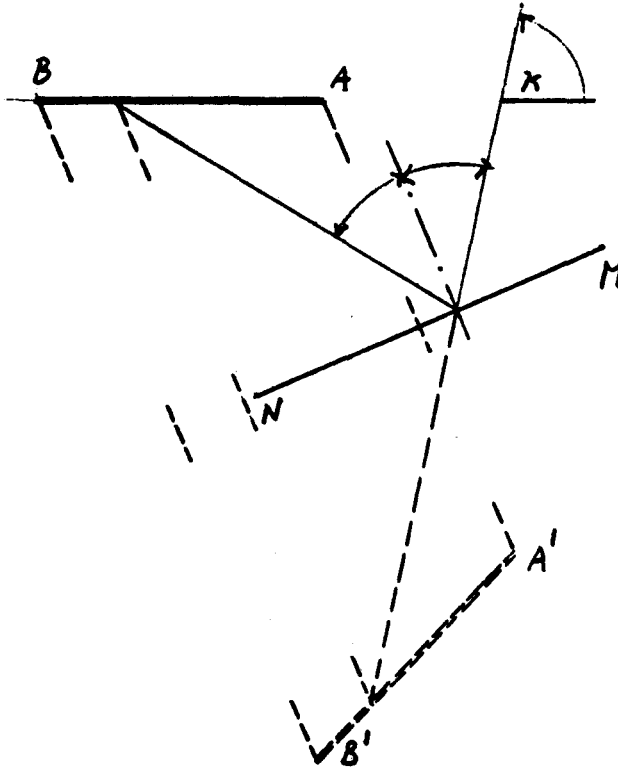
The reflector is hit by rays between $U_R^{(R)}$ and $U_A^{(R)}$ (if $T_L \leq T_A$) or S (if $T_L > T_A$), respectively.

$$I_d(\kappa) = \begin{cases} T_R - T_M & \text{for } T_L \geq T_B \\ T_R - T_M + T_B - T_L & \text{for } T_L < T_B \\ 0 & \text{otherwise} \end{cases}$$

which is indeed the sum of the widths of the incident ray bundles.

3.3 Reflection at the Line Segment

Now, we have to determine which part of the rays hitting the reflector will be reflected to the under side of the collector. The necessary calculations have to be carried out separately for each section of the reflector. At first we consider the case of the line segment. Instead of examining the reflection at the straight line, it is as well possible to reflect the collector at the imaginary extension of the line segment and to check which rays (without reflection) meet this reflected collector.



The head and the end of the reflected collector are determined from the following transformation

$$A' = m A + v$$

$$B' = m B + v$$

where m is a 2×2 matrix with the elements

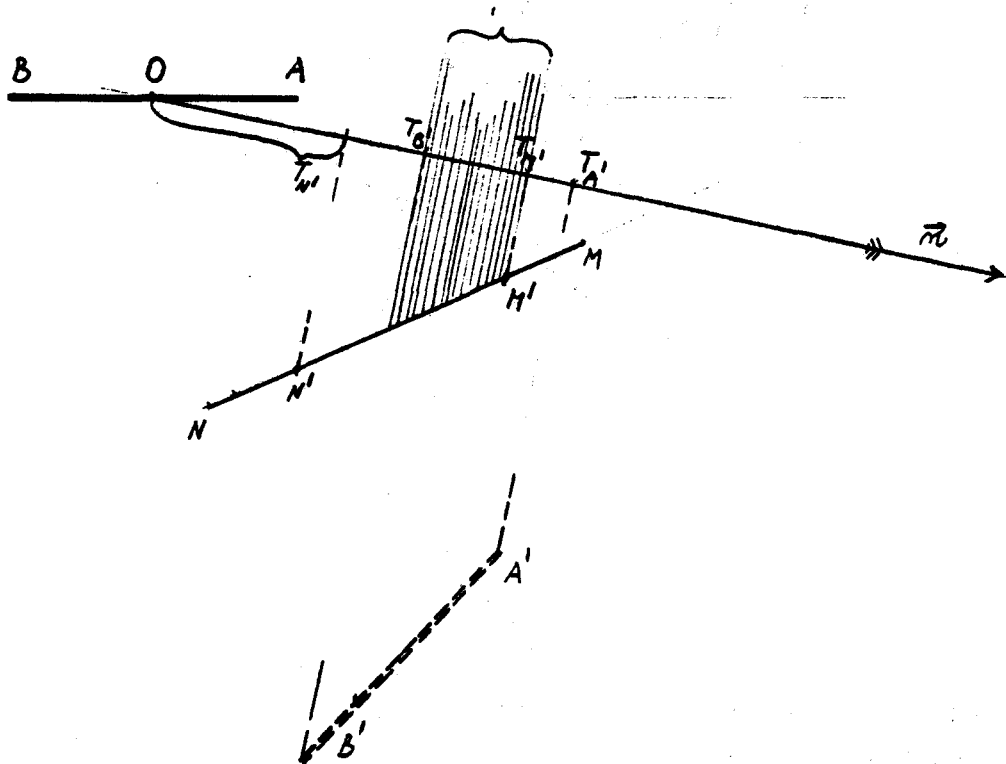
$$m_{11} = -m_{22} = \frac{(x_M - x_N)^2 - (y_M - y_N)^2}{(x_M - x_N)^2 + (y_M - y_N)^2}$$

$$m_{12} = m_{21} = \frac{2(x_M - x_N) \cdot (y_M - y_N)}{(x_M - x_N)^2 + (y_M - y_N)^2}$$

and v is the vector

$$v = 2 \frac{x_N y_M - y_N x_M}{(x_M - x_N)^2 + (y_M - y_N)^2} \begin{pmatrix} y_M - y_N \\ x_M - x_N \end{pmatrix}$$

To find the illuminated parts of the reflected collector the same procedure as before is used. The segment MN of the reflector is assumed to be illuminated between the points M' and N' . A straight line is drawn through O perpendicular to the direction of the incident rays; the direction of this line is $\bar{n} = (\sin \kappa, -\cos \kappa)$.



The points A' , B' , M' , N' are projected onto this straight line in the direction of incidence; the projections are scalar products, e.g.

$$T_{A'} = A' \cdot \bar{n}$$

where $T_{A'}$ is the coordinate on the straight line. Now, only the relative positions of these points T on the straight line have to be discussed.

Different cases have to be considered:

1) $T_{B'} \geq T_{A'}$:

No ray hits the collector.

2) $T_{B'} < T_{A'}$:

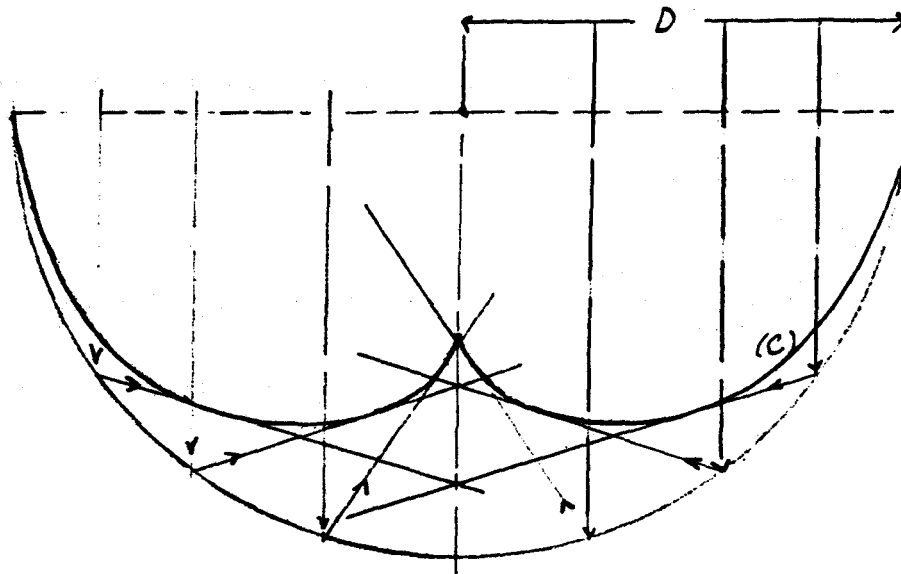
If moreover $T_{M'} \leq T_{B'}$ or $T_{A'} \leq T_{N'}$, no ray hits the collector.

Otherwise the section between maximum $(T_{N'}, T_{B'})$ and minimum $(T_{M'}, T_{A'})$ is illuminated.

The flux is proportional to the width of the respective ray bundle, i.e. $|\min(T_{M'}, T_{A'}) - \max(T_{N'}, T_{B'})|$.

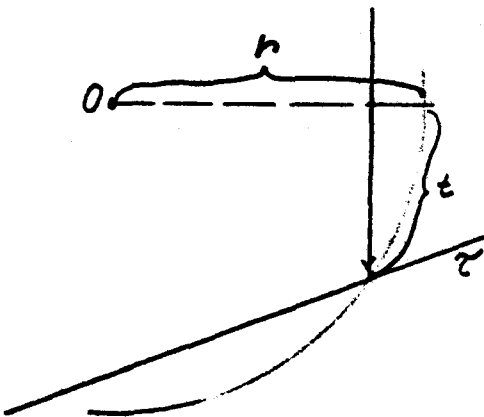
3.4 Reflection at the Circular Arc

Equivalent investigations have to be carried out for the case of the circular arc. If the light comes from a definite direction to a circular arc, all reflected rays are tangents of a specific curve: the envelope curve or caustic.



We confine ourselves to the rays of region D; therefore we need only to consider the segment c of the caustic. Now the tangent from any point X to c has to be found. The main task of all considerations is to find a reliable and fast procedure for this purpose which will finally decide about the usefulness of the computer program. Difficulties arise mainly from the fact that, depending on the position of X , either none, one or two tangents or one double tangent to segment c of the caustic may exist and it has to be decided upon, which can be used. i.e. which intersects the circle within the region D.

We choose the centre of the circle as origin. A point on the periphery is characterized as $T = (r \cos t, -r \sin t)$ with parameter t .



The ray hitting in T will be reflected in the direction of the straight line

$$\tau: y \sin 2t - x \cos 2t + r \cos t = 0 \quad (*)$$

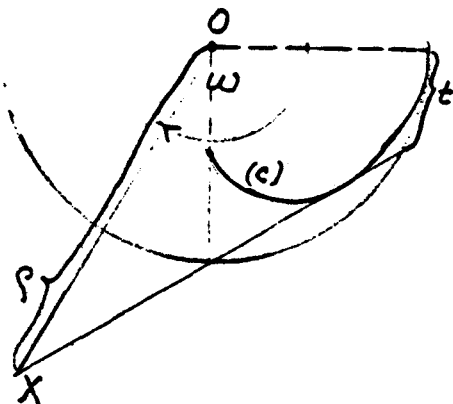
The equation of the caustic (to which τ is a tangent) is

$$x = r \cos^3 t$$

$$y = r(\sin^3 t - \frac{3}{2} \sin t) \quad \text{or, after eliminating } t,$$

$$y = -r \left[\frac{1}{2} + \left(\frac{x}{r} \right)^{2/3} \right] \sqrt{1 - \left(\frac{x}{r} \right)^{2/3}}$$

A point X is assumed and the tangent from X to the caustic has to be found.



The coordinates of X are:

$$(\rho \cos \omega, -\rho \sin \omega). \quad (**)$$

For the intersection of the tangent with the circle we obtain from (*) and (**) the equation

$$-\rho \sin \omega \sin 2t - \rho \cos \omega \cos 2t + r \cos t = 0$$

and, respectively,

$$\rho \cos(2t-\omega) = r \cos t .$$

If we insert $x = \cos t$, we find

$$\rho \cos \omega (2x^2 - 1) + 2\rho \sin \omega \cdot x \sqrt{1-x^2} = rx .$$

In order to find the "correct" solution of the equation, different ranges of ω will be distinguished:

$$1) \quad \frac{\pi}{2} < \omega < \frac{3\pi}{2}$$

In this case further distinctions are made for different orders of magnitude of ρ . For $\rho = \infty$, $\rho = 0$ and $\rho = r$ the solution can be given directly. In the neighbourhood of this solution the equation will be expanded in a small parameter. From only a few terms of the expansion the solution can be calculated. For the first case ($\rho > r$), we write the equation as follows:

$$\cos(2t-\omega) = \frac{r}{\rho} \cos t .$$

For $\rho \rightarrow \infty$ (Fig. 12)

$$\cos(2t-\omega) = 0$$

and from this the solution results: $t = \frac{\omega}{2} - \frac{\pi}{4} .$

For large values we use $t = \frac{\omega}{2} - \frac{\pi}{4} + T$ and obtain the equation

$$\cos(-\frac{\pi}{2} + 2T) = \frac{r}{\rho} \cos(\frac{\omega}{2} - \frac{\pi}{4} + T)$$

or

$$2 \sin T \cos T = \frac{r}{\rho} \cos(\frac{\omega}{2} - \frac{\pi}{4}) \cos T - \sin(\frac{\omega}{2} - \frac{\pi}{4}) \sin T .$$

With the abbreviations $\sin T = x$, $\cos T = \sqrt{1-x^2}$,

$\frac{r}{\rho} = \epsilon$, $\cos(\frac{\omega}{2} - \frac{\pi}{4}) = a$ and $\sin(\frac{\omega}{2} - \frac{\pi}{4}) = b$, this results in

$$\sqrt{1-x^2} (2x - \epsilon a) = -\epsilon b x .$$

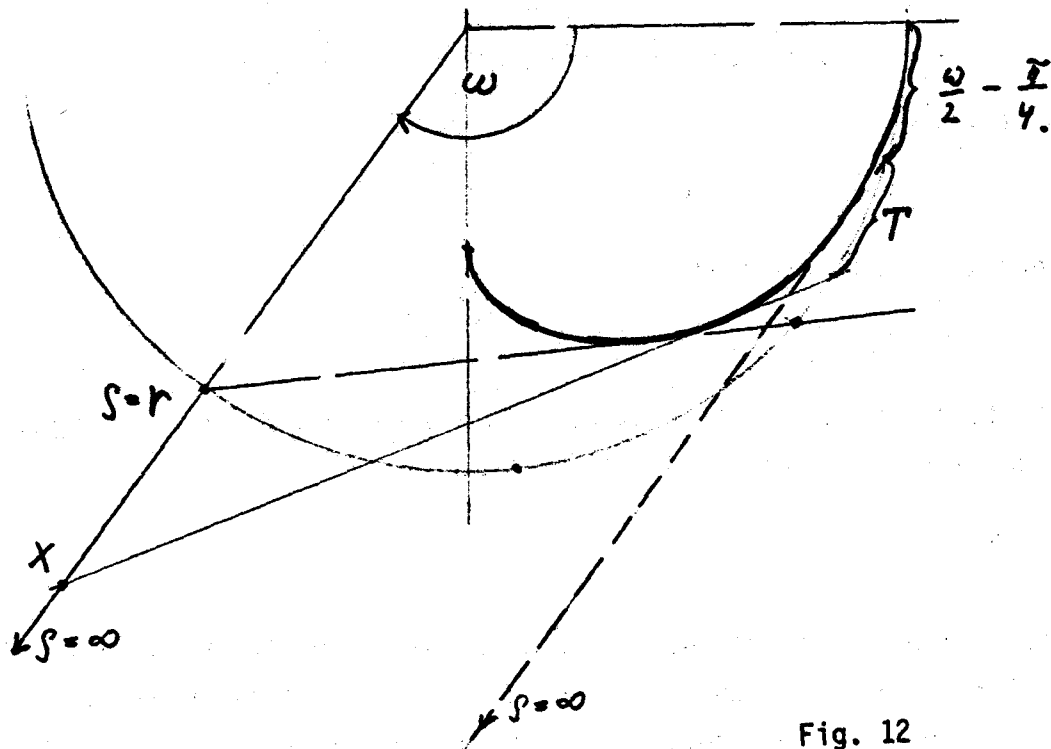


Fig. 12

If x is expanded with the small parameter ϵ ,

$$x = \frac{a}{2} \epsilon (1 + a_1 \epsilon + a_2 \epsilon^2 + \dots),$$

after insertion and comparison of the respective coefficients one finds

$$T = \arcsin \left\{ a \frac{\epsilon}{2} \left[1 - b \frac{\epsilon}{2} + b^2 \left(\frac{\epsilon}{2} \right)^2 - \left(\frac{1}{2} a^2 b + b^3 \right) \left(\frac{\epsilon}{2} \right)^3 + (b^4 + 2a^2 b^2) \left(\frac{\epsilon}{2} \right)^4 + \dots \right] \right\}$$

In the second case one obtains from $\frac{\rho}{r} \cos(2t - \omega) = \cos t$ ($\rho \ll r$) for $\rho \rightarrow 0$ the solution $t = \frac{\pi}{2}$. From the equation $t = \frac{\pi}{2} - T$ and analogous considerations as above one obtains with $a = \cos \omega$, $b = \sin \omega$, $\epsilon = \frac{\rho}{r}$:

$$T = \arcsin \left\{ -a \epsilon \left[1 + 2b \epsilon + (4b^2 - 2a^2) \epsilon^2 + (8b^3 - 13a^2 b) \epsilon^3 + \dots \right] \right\}$$

The third case ($\rho \sim r$) yields for $\rho = r$ the equation $\cos(2t - \omega) = \cos t$ and, hence, the solution $t = \frac{\omega}{3}$. From the equation $t = \frac{\omega}{3} + T$ follows

$$T = \arcsin \left\{ -\frac{a}{3b} (\epsilon - 1) \left[1 - \left(\frac{3}{2} \left(\frac{a}{3b} \right)^2 + \frac{2}{3} \right) (\epsilon - 1) + \left(\frac{9}{2} \left(\frac{a}{3b} \right)^4 + \frac{4}{3} \left(\frac{a}{3b} \right)^2 + \frac{4}{9} \right) (\epsilon - 1)^2 + \dots \right] \right\}$$

with

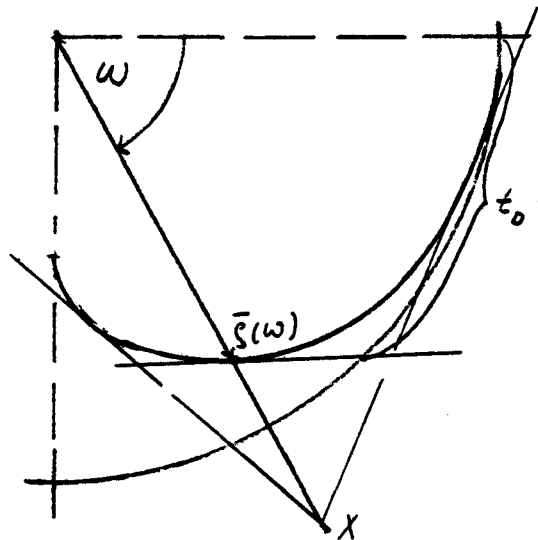
$$a = \cos \frac{\omega}{3}, \quad b = \sin \frac{\omega}{3}, \quad \varepsilon = \frac{\rho}{r}.$$

Consequently, there is always one tangent in this range of ω .

$$2) \quad 0 < \omega < \frac{\pi}{2}$$

Here three cases are possible: no tangent, two tangents, one double tangent.

We speak of a double tangent if, in case that the point X is approaching the caustic, two tangents coincide.



At first, the intersection of the ray through the centre with angle ω to the horizontal with the caustic is determined. The result is an equation of third degree to be solved by means of the formula of Cardani.

With

$$x = \frac{1}{\sqrt[3]{\cos \omega}} \left(\frac{2}{3} \sin \omega + \frac{10}{81} \sin^3 \omega \right) \quad \text{for } 0 \leq \omega \leq 0,01$$

$$x = \frac{1}{\sqrt[3]{\cos \omega}} \left(\sqrt[3]{1+\sin \omega} - \sqrt[3]{1-\sin \omega} \right) \quad \text{for } 0,01 < \omega < \frac{\pi}{2}$$

it follows

$$\bar{\rho}(\omega) = \frac{r}{2} \sqrt{\frac{4+x^2}{1+x^2}}$$

and for the tangent parameter

$$t_D = \arctan x .$$

The first expression for x is used to avoid the cancellation in the exact second formula for small values of ω .

By $\bar{\rho}$ different ranges and cases can be distinguished.

a) For a point X with $\rho < \bar{\rho}(\omega)$, there is no tangent to the caustic.

b) For $\bar{\rho} \leq \rho \leq \frac{\rho+r}{2}$, we are "near the double tangent" (Fig. 13).

The two conditions are valid:

$$\bar{\rho} \cos(2t_D - \omega) = r \cos t_D \quad (*)$$

$$2\bar{\rho} \sin(2t_D - \omega) = r \sin t_D .$$

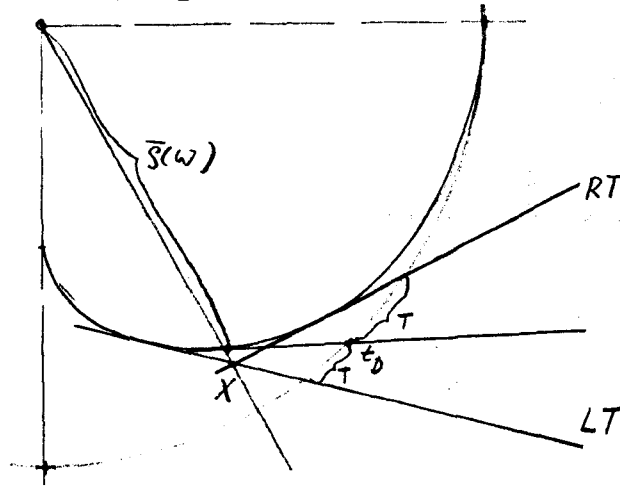


Fig. 13

If we write $t_D = t_D + T$, we obtain the equation for determining t_D and T , respectively:

$$0 = \rho \cos(2t_D - \omega) - r \cos t_D = [(\rho - \bar{\rho}) + \bar{\rho}] \cos(2t_D + 2T - \omega) - r \cos(t_D + T)$$

or, using (*)

$$\begin{aligned} 0 &= [(\rho - \bar{\rho}) + \bar{\rho}] (\cos 2T \cos(2t_D - \omega) - \sin 2T \sin(2t_D - \omega)) - r(\cos t_D \cos T - \sin t_D \sin T) = \\ &= [(\rho - \bar{\rho}) + \bar{\rho}] \left(\frac{r}{\rho} \cos 2T \cos t_D - \frac{r}{2\rho} \sin 2T \sin t_D \right) - r(\cos t_D \cos T - \sin t_D \sin T) \end{aligned}$$

$\sin T$ and $\cos T$ are now expanded in T . If the expansion is terminated after 3 terms, one obtains a quadratic equation for T . The solution for the right

hand tangent RT is

$$t_{OR} = \begin{cases} t_D - \sqrt{\rho - \bar{\rho}} \frac{\sqrt{\rho - \bar{\rho}} \sin t_D + \sqrt{(\rho - \bar{\rho}) \sin^2 t_D + 2(4\rho - \bar{\rho}) \cos^2 t_D}}{(4\rho - \bar{\rho}) \cos t_D} & \text{for } 0 \leq \omega \leq \frac{\pi}{2} - 0,2 \\ \arcsin \frac{r}{2\rho} & \text{for } \frac{\pi}{2} - 0,2 \leq \omega \leq \frac{\pi}{2} \end{cases}$$

and for the left-hand tangent LT

$$t_{OL} = \min \left\{ \frac{\pi}{2}, t_D - \sqrt{\rho - \bar{\rho}} \frac{\sqrt{\rho - \bar{\rho}} \sin t_D - \sqrt{(\rho - \bar{\rho}) \sin^2 t_D + 2(4\rho - \bar{\rho}) \cos^2 t_D}}{(4\rho - \bar{\rho}) \cos t_D} \right\}$$

c) In the range $\frac{\rho+r}{2} \leq \rho \leq \min(k \cdot r, \frac{1+2 \cos \omega}{3 \cos \omega} r)$, t_0 for the right-hand tangent is given by

$$t_0 = \frac{\omega}{2} + \arcsin \left\{ -\frac{a}{3b}(\epsilon-1) \left[1 - \left(\frac{3}{2} \left(\frac{a}{3b} \right)^2 + \frac{2}{3} \right) (\epsilon-1) + \dots \right] \right\},$$

$$a = \cos \frac{\omega}{3}, \quad b = \sin \frac{\omega}{3}, \quad \epsilon = \frac{\rho}{r}.$$

For accuracy reasons k has been chosen as 1.4 in this case. For the left-hand tangent the values are $k = 1.5$ and $t_0 = \omega$.

d) For points X with $\rho \geq \min(1.4 r, \frac{1+2 \cos \omega}{3 \cos \omega} r)$ obviously $t_0 = 0$ results for the right-hand tangent. We obtain, correspondingly, for the left-hand tangent in the range $1.5 r \leq \rho \leq \frac{1}{\cos \omega}$:

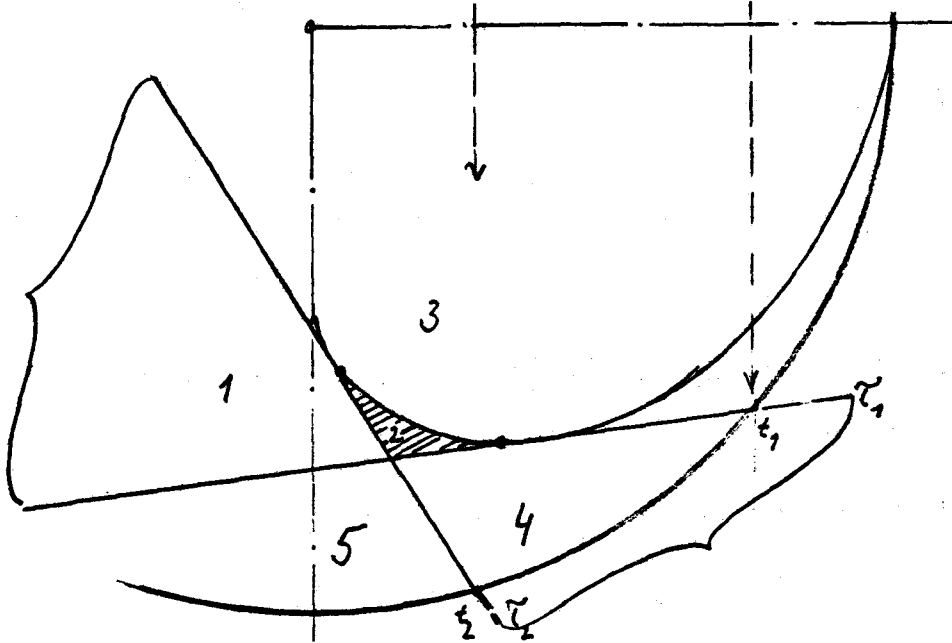
$$t_0 = \frac{\omega}{2} + \frac{\pi}{4} - \arcsin \left\{ \frac{a}{2} \epsilon \left[1 + \frac{b}{2} \epsilon + \left(\frac{b}{2} \right)^2 \epsilon^2 + \dots \right] \right\}$$

$$a = \cos\left(\frac{\omega}{2} + \frac{\pi}{4}\right), \quad b = \sin\left(\frac{\omega}{2} + \frac{\pi}{4}\right), \quad \epsilon = \frac{r}{\rho}.$$

For the ρ -values in the remaining ranges, the determination of tangents is not necessary since the tangents will not appear because of the possible reasonable location of collector and reflector.

The values t_0 and T determined up till now are not the exact intersection points between the tangents and the circle but are only first guesses for a Newton-method to be applied to the original equations.

3.5 Tangent Regions



Let t_1 and t_2 be two parameter values corresponding to points of the circle. The corresponding tangents to the caustic are given by

$$\tau_i \equiv y \sin 2 t_i - x \cos 2 t_i + r \cos t_i = 0 \quad .$$

By these tangents and their point of contact with the caustic five regions are determined:

$$1) \quad \tau_1 \geq 0 \quad \text{and} \quad \tau_2 \leq 0 \quad ;$$

$$2) \quad \tau_1 > 0 \quad \text{and} \quad \tau_2 > 0 \quad \text{and} \quad r \cos^3 t_2 \leq x \leq r \cos^3 t_1$$

$$\text{and} \quad y \leq r \left[\frac{1}{2} + \left(\frac{x}{r} \right)^{2/3} \right] \sqrt{1 - \left(\frac{x}{r} \right)^{2/3}}$$

$$3) \quad \tau_1 > 0 \quad \text{and} \quad \tau_2 > 0 \quad \text{without the constraints of 2) with respect to } x \text{ and } y;$$

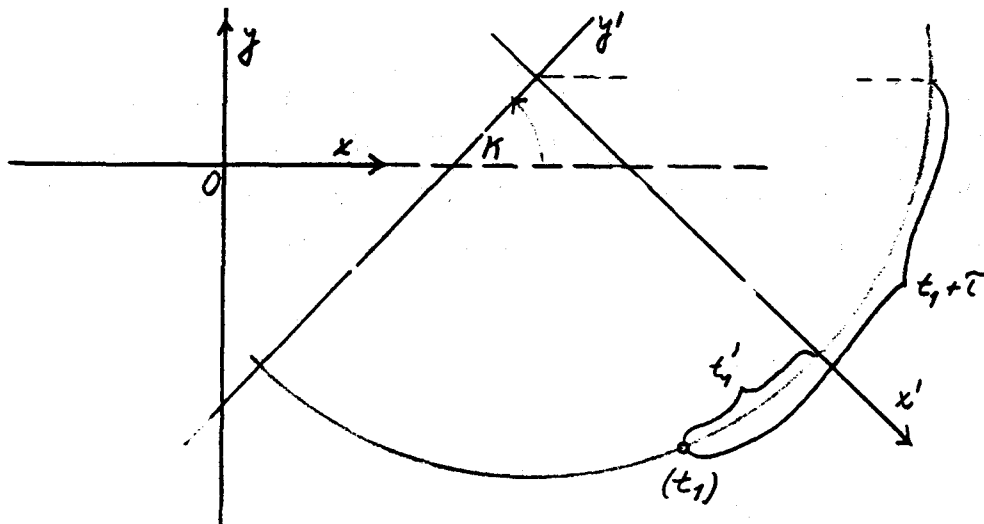
$$4) \quad \tau_1 \leq 0 \quad \text{and} \quad \tau_2 > 0 \quad ;$$

$$5) \quad \tau_1 \leq 0 \quad \text{and} \quad \tau_2 < 0 \quad .$$

In this way we are able to decide for any point of the plane in which of the five regions it is located.

3.6 Transformation

As for the considerations concerning the circular arc we had left our original coordinate system (collector centre as origin) and had chosen the centre of the circle as origin, we have to carry out a suitable coordinate transformation depending on the angle of incidence of the rays.



The transformation of coordinates is as follows:

$$x' = x \sin \kappa - y \cos \kappa + [-m_1 \sin \kappa + m_2 \cos \kappa]$$

$$y' = x \cos \kappa + y \sin \kappa + [-m_1 \cos \kappa - m_2 \sin \kappa]$$

By this the points A, B and S and the initial and end points t_1 , t_2 of the illuminated arc are transformed.

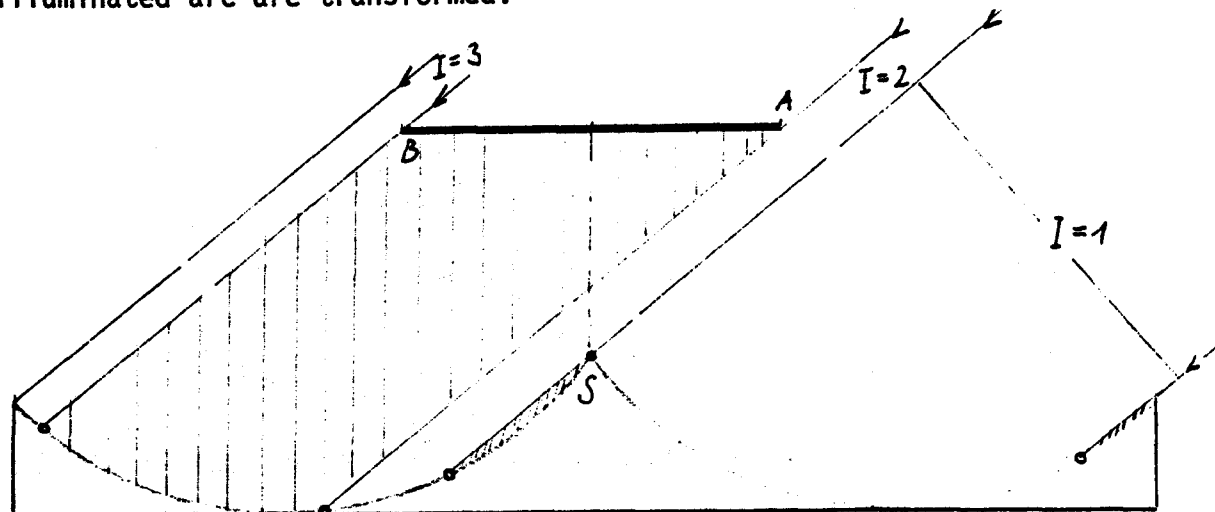


Fig. 14

$$t_1' = \frac{3}{2} \pi - (t_2 + \tau + \kappa) ,$$

$$t_2' = \frac{3}{2} \pi - (t_1 + \tau + \kappa) ,$$

with the additional conditions

$$t_2' = \frac{\pi}{2} , \quad \text{if } t_2' > \frac{\pi}{2} ,$$

and

$$t_1' = \frac{t_2}{3} , \quad \text{if } t_1' < \frac{t_2}{3} .$$

Depending on the location of the point S, it is possible that once reflected rays do not meet the collector but hit again the reflector. This leads to a further limitation of the parameter range between t_1 and t_2 in which the incident rays are reflected onto the collector. This consideration is necessary only for the cases $I = 1$ and $I = 3$. The possible new parameter values are obtained by determination of tangents of the caustic passing through the point S. In detail, the following values are obtained depending on the position of the point S (ranges 1 to 5):

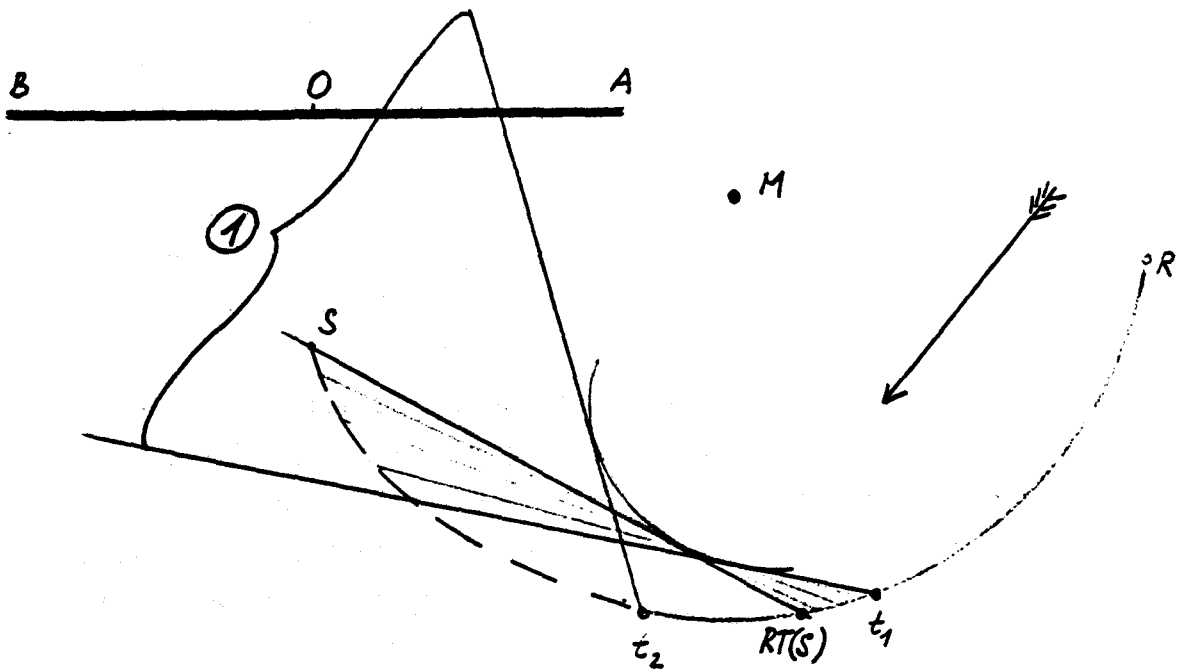
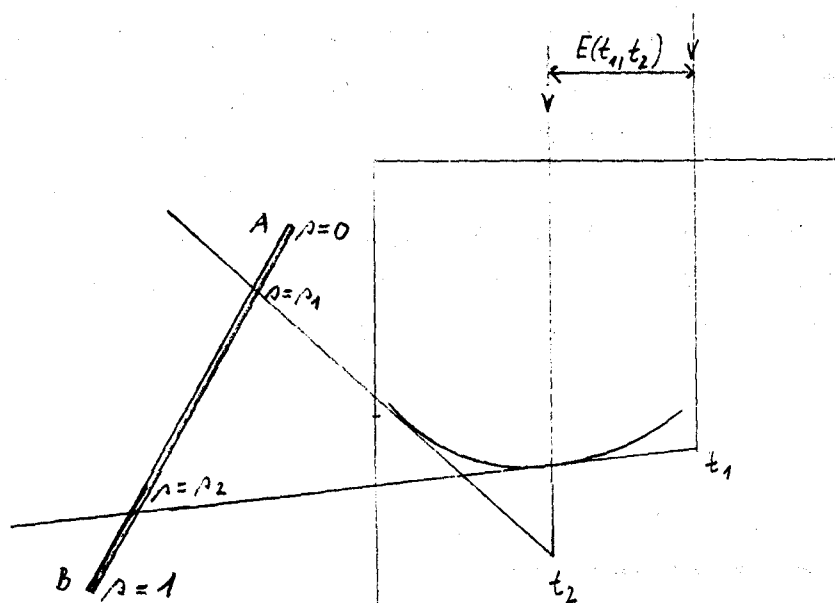


Fig. 15

- S in range 1): $t_1 = RT(S, r)$; t_2 unchanged (Fig. 15)
 S in range 2): $t_1 = RT(S, r)$; $LT(S, r)$
 S in range 3): t_1 and t_2 coincide, i.e. no reflection
 S in range 4): t_1 unchanged; $t_2 = LT(S, r)$
 S in range 5): t_1 and t_2 unchanged.

The ranges 1) to 5) are now redetermined with the new values for t_1 , t_2 .

3.7 Determination of flux



If all rays hitting the reflector between t_1 and t_2 are reflected to the collector, the flux is proportional to the width $E(t_1, t_2) = r|\cos t_1 - \cos t_2|$.

This case will not always prevail; it will rather depend on the position of the collector with respect to the reflector. As can easily be seen from the sketch, everything depends on the fact in which of the ranges 1) to 5) the initial and end points of the collector are located. Therefore, at first, the intersection points s_i of the limiting tangents through t_1 and t_2 with the straight line of the collector are determined, the straight line being described parametrically by $X = A + s(B-A)$. The points of the collector correspond to the parameter values s between 0 and 1.

The required points of intersection are given by

$$s_i = \frac{r \cos t_i + b_2 \sin 2t_i - b_1 \cos 2t_i}{(a_1 - b_1) \cos 2t_i - (a_2 - b_2) \sin 2t_i} \quad (i = 1, 2)$$

If the absolute value of the denominator is very small, e.g. smaller than a given number σ , tangent and collector are nearly in parallel, and we put $s_i = -1$. Investigating such possible collector positions, one has to consider that the reflected rays may only hit the collector from below. This brings a limitation of the reasonable possibilities. If, for instance, both intersection points lie on the collector ($0 < s_1, s_2 < 1$), B can only be situated in range 5) and A only in 2) or 3). If B in 1) and A in 4), for instance, the reflected rays would hit the upper side. We determine the reasonable cases.

- 1) $0 \leq s_1, s_2 \leq 1$, i.e. both intersections lie on the collector. B can only be located in 5). If then A lies in 3), the value of the flux is $\epsilon = E(t_1, t_2)$.

If A is in 2), it is to be seen from Fig. 16 that ϵ consists of two parts, $\epsilon = E(t_1, RT(A)) + E(LT(A), t_2)$.

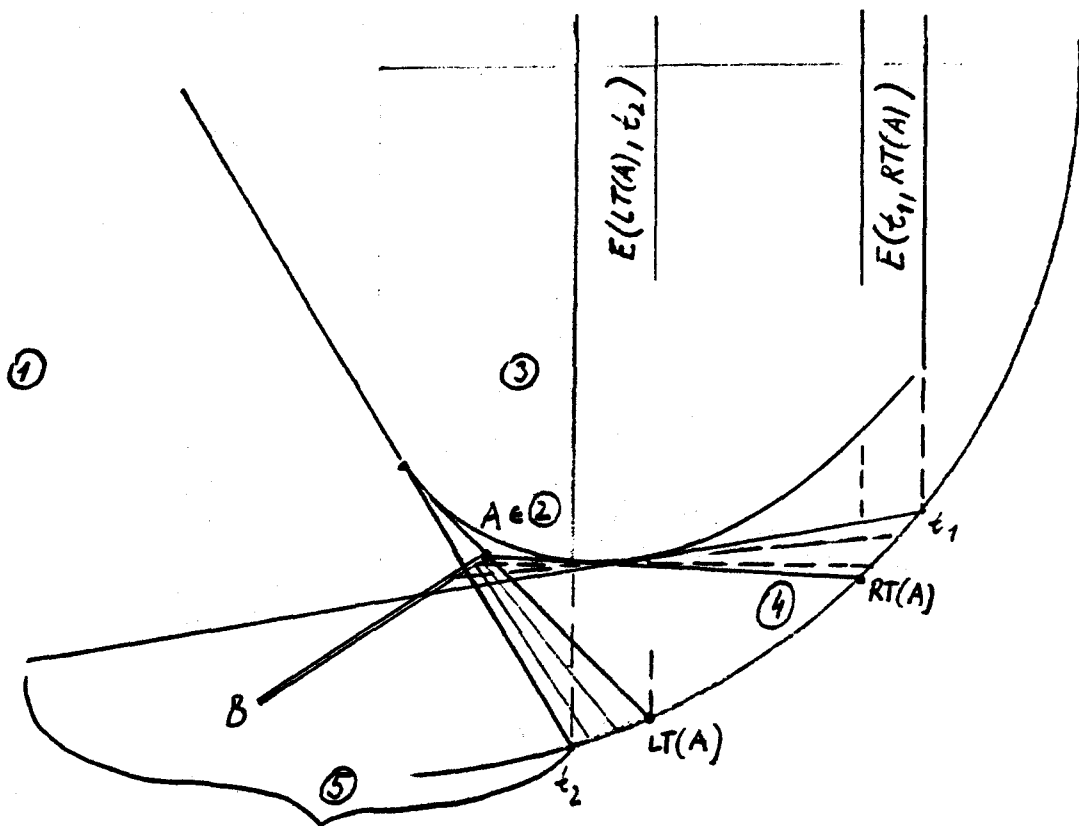


Fig. 16

2) Only one intersection point on the collector:

a) If B is in 1), one gets for A in 2)

$$\epsilon = E(RT(B,r), RT(A,r)) + E(LT(A,r), t_2)$$

and for A in 3)

$$\epsilon = E(RT(B,r), t_2) \quad (\text{Fig. 17}) .$$

b) If B is in 4), one gets for A in 2)

$$\epsilon = E(t_1, RT(A,r)) + E(LT(A,r), LT(B,r))$$

and for A in 3)

$$\epsilon = E(t_1, LT(B,r)) .$$

c) If B is in 5) one gets for A in 1)

$$\epsilon = E(t_1, RT(A,r))$$

and for A in 4)

$$\epsilon = E(LT(A,r), t_2) .$$

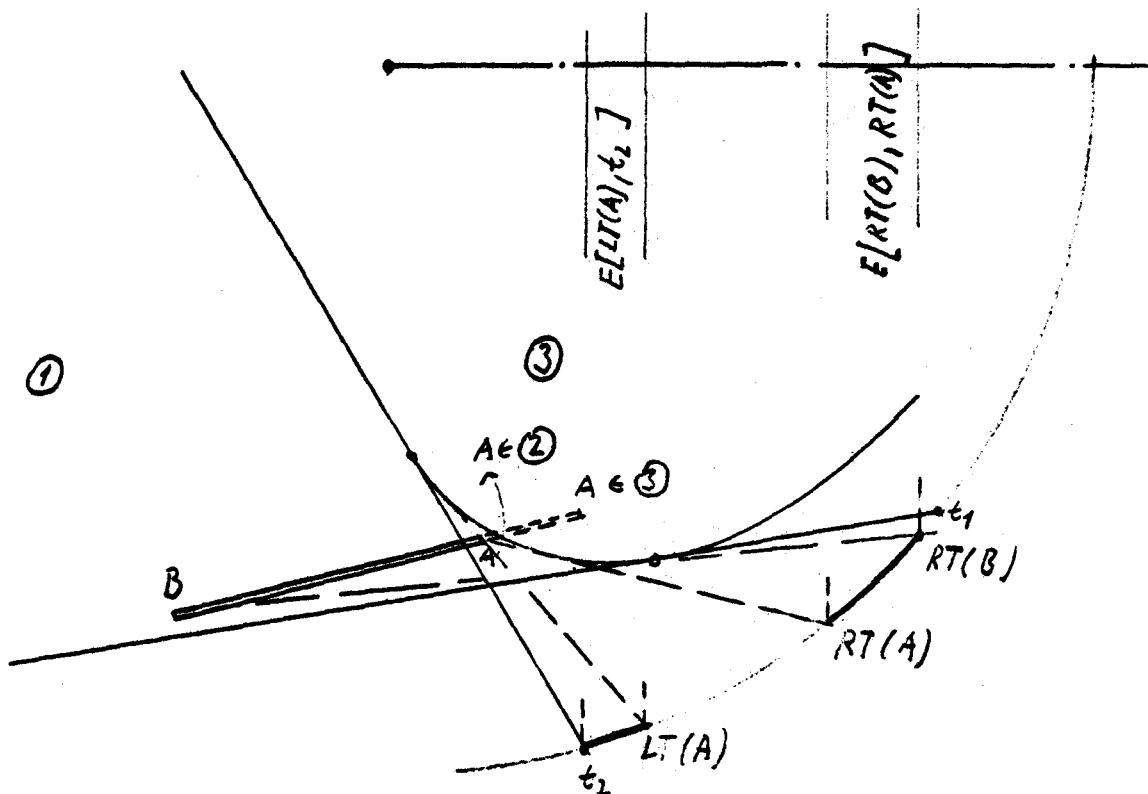


Fig. 17

3) Both intersection points outside the collector:

a) If B in 1), then $\epsilon = E(RT(B,r), RT(A,r))$

b) If B in 2), then

for A in 2) $\epsilon = E(RT(B,r), RT(A,r)) + E(LT(A,r), LT(B,r))$

and for A in 3) $\epsilon = E(RT(B,r), LT(A,r))$

c) If B in 3) or 5), then $\epsilon = 0$

d) If B in 4), then $\epsilon = E(LT(A,r), LT(B,r))$.

$E(p,k)$ is always an abbreviation for $r \cos|p - \cos k|$.

4. FLUX PER UNIT AREA

Till now we only investigated the total flux impinging on the underside of the collector. To avoid too large temperature variations over the collector the flux per unit area has to be considered.

We assume the curve of the reflector to have all mathematical properties which are necessary for the following considerations (The notations are shown in Fig. 18

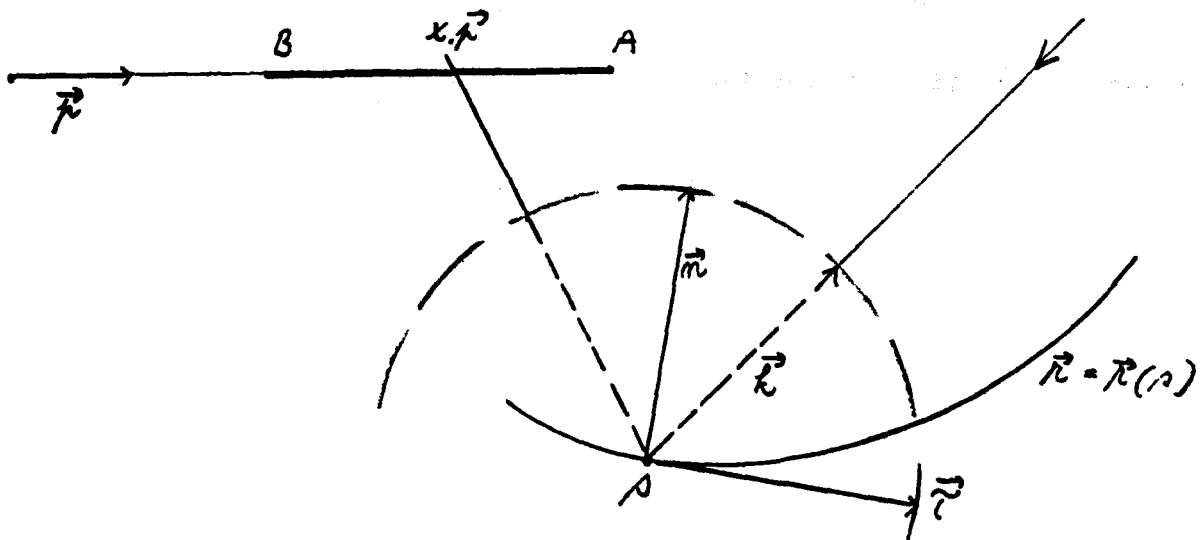


Fig. 18

\vec{p} is a unit vector in the direction of the collector. The curve of the reflector is represented as $\vec{r} = \vec{r}(s)$ with the arc length s as parameter. \vec{k} is a unit vector in the direction of the incoming sun rays, the tangent \vec{t} and \vec{n} normal to $\vec{r} = \vec{r}(s)$ describe a local coordinate system in the point s . Every point of the reflector corresponds with a point x on the collector where the ray reflected in s hits the collector. This correspondence can be written as a mapping $x = f(s)$. To construct this mapping we decompose the vector \vec{k} as

$$\vec{k} = k_1 \vec{t} + k_2 \vec{n}$$

From Fig. 18 it follows

$$x \vec{p} = \vec{r}(s) + h(-k_1 \vec{t} + k_2 \vec{n})$$

Scalar multiplication with $k_2\vec{\tau} + k_1\vec{n}$ yields

$$x = f(s) = \frac{k_2(\vec{r} \cdot \vec{\tau}) + k_1(\vec{r} \cdot \vec{n})}{k_2(\vec{p} \cdot \vec{\tau}) + k_1(\vec{p} \cdot \vec{n})} = \frac{(\vec{k} \cdot \vec{n})(\vec{r} \cdot \vec{\tau}) + (\vec{k} \cdot \vec{\tau})(\vec{r} \cdot \vec{n})}{(\vec{k} \cdot \vec{n})(\vec{p} \cdot \vec{\tau}) + (\vec{k} \cdot \vec{\tau})(\vec{p} \cdot \vec{n})}.$$

Since we have expressed $f(s)$ as a combination of scalar products, this mapping is invariant with respect to linear transformations, i.e. changes of the coordinate system.

After these general considerations we can calculate the flux per unit area $\rho(x)$. With the notations of Fig. 19 we have

$$\Delta E = (\vec{k} \cdot \vec{n}) \Delta s = \rho(x) \Delta x$$

$$\rho(x) = (\vec{k} \cdot \vec{n}) \frac{1}{\frac{\Delta x}{\Delta s}}$$

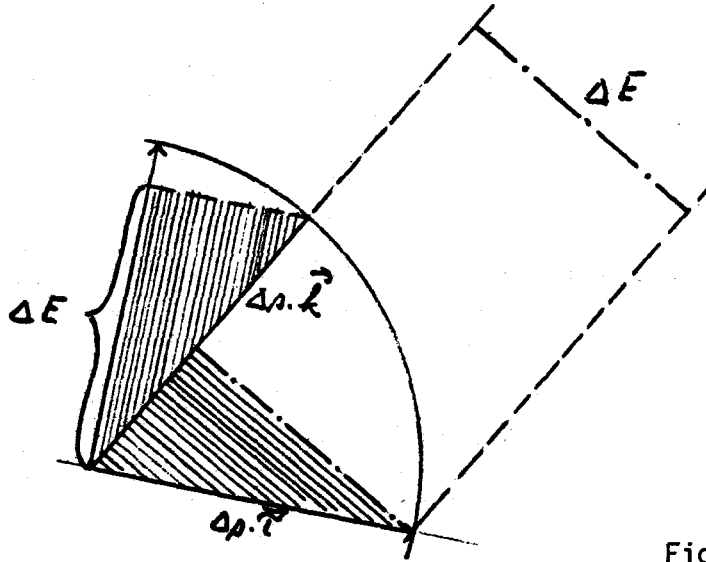


Fig. 19

and as limit for $\Delta s \rightarrow 0$

$$\rho(x) = \frac{\vec{k} \cdot \vec{n}}{f'(s)}.$$

We now apply this result to the special case, where the reflector has the shape of a circular arc given by

$$\vec{r}(t) = M + r [\cos(t+\tau), -\sin(t+\tau)] .$$

Since here the parameter t is different from the arc length, the formula for $\rho(s)$ must be modified to

$$\rho(x) = \frac{\vec{k} \cdot \vec{h}}{\frac{d\vec{f}}{dt} \cdot \frac{d\vec{t}}{ds}} .$$

To construct the mapping $x = f(t)$ we need the vectors

$$\vec{k} = [\cos \kappa, \sin \kappa] , \quad \vec{p} = [1, 0] ,$$

$$\vec{\tau} = [-\sin(t+\tau), -\cos(t+\tau)] , \quad \vec{h} = [-\cos(t+\tau), \sin(t+\tau)]$$

and the scalar products

$$\vec{k} \cdot \vec{\tau} = -\sin(t+\tau+\kappa) , \quad \vec{k} \cdot \vec{h} = -\cos(t+\tau+\kappa) ,$$

$$\vec{r} \cdot \vec{\tau} = -x_M \sin(t+\tau) - y_M \cos(t+\tau) , \quad \vec{r} \cdot \vec{h} = -x_M \cos(t+\tau) + y_M \sin(t+\tau) - r .$$

Then we have

$$x = f(t) = x_M + \frac{y_M \cos(2(t+\tau)+\kappa) + r \sin(t+\tau+\kappa)}{\sin(2(t+\tau)+\kappa)}$$

and for the derivative

$$\frac{dx}{dt} = \frac{r [\cos(t+\tau+\kappa) \sin(2(t+\tau)+\kappa) - 2 \sin(t+\tau+\kappa) \cos(2(t+\tau)+\kappa)] - 2y_M}{\sin^2(2(t+\tau)+\kappa)}$$

For the circle the relation between the parameters s and t is $s = rt$,

and the derivative is $\frac{dt}{ds} = \frac{1}{r}$.

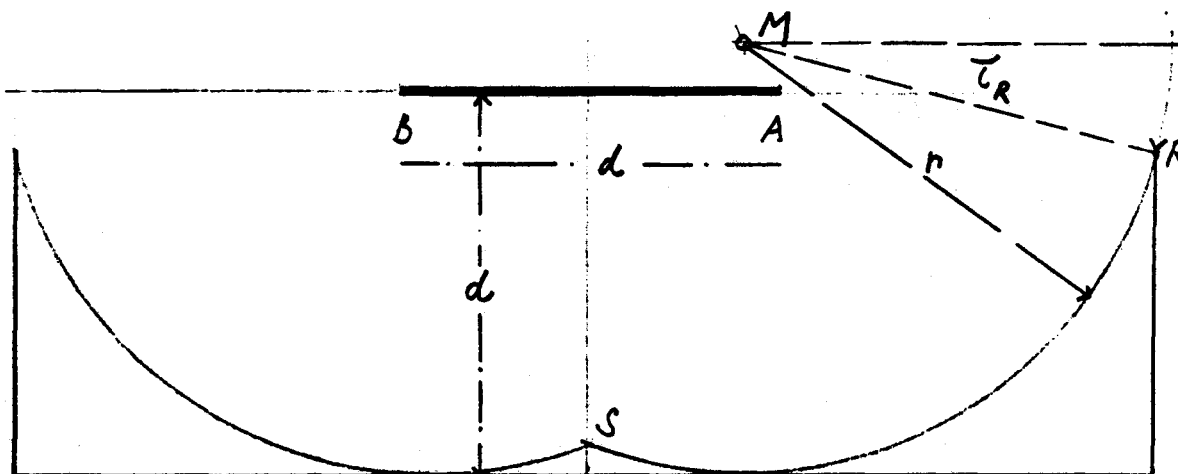
Inserting all this into the formula for ρ , we arrive at

$$\rho(x) = \frac{-r \cos(t+\tau+\kappa) \sin^2(2(t+\tau)+\kappa)}{r [\cos(t+\tau+\kappa) \sin(2(t+\tau)+\kappa) - 2 \sin(t+\tau+\kappa) \cos(2(t+\tau)+\kappa)] - 2y_M} ;$$

x is the coordinate on the collector, t the parameter on the circular reflector.

5. AN EXAMPLE

As an example for the previously outlined method of solution we look for the "best" reflector consisting of two circular arcs.



The notations are as in the illustration; $d = 2$; $A = (1,0)$ and $B = (-1,0)$ are the endpoints of the collector; the right circular arc is uniquely determined by the centre M and the endpoints R and S . S is also the point of symmetry of the reflector. The height d being fixed by the condition that the reflector touches the ground, we search for the parameters corresponding to given y_S and y_R .

At first, we derive an auxiliary quantity h :

$$h = \frac{x_R^2 + (y_R - y_S)(y_R - d)}{x_R \sqrt{y_S - d} + \sqrt{y_R - d} \sqrt{x_R^2 + (y_R - y_S)^2}}.$$

The parameters of the reflector are

$$x_M = h \sqrt{y_S - d}, \quad y_M = \frac{d + y_S}{2} + \frac{1}{2} h^2, \quad r = y_M - d,$$

$$\tau_R = \arctan \frac{y_M - y_R}{x_R - x_M}, \quad \tau_L = \arccos \frac{x_M}{r}.$$

Now we can assign the input matrices D_R , D_L ; of course, we have to take care that the angular parameter of the circular arc does not exceed $\frac{\pi}{2}$; eventually we must describe such a segment by two matrix rows.

We distinguish 3 cases:

$$1) \quad \pi - \tau_L - \tau_R \leq \frac{\pi}{2}$$

Here D_R and D_L are

$$D_R = (x_M, y_M, r, \tau_R, 0, \pi - \tau_L - \tau_R, 0)$$

$$D_L = (-x_M, y_M, r, \tau_L, 0, \pi - \tau_L - \tau_R, 0)$$

$$2) \quad \frac{\pi}{2} < \pi - \tau_L - \tau_R \leq \frac{\pi}{2} + \Delta \quad \text{with} \quad \Delta = 0,05$$

To avoid numerical difficulties, this case is excluded.

$$3) \quad \frac{\pi}{2} + \Delta < \pi - \tau_L - \tau_R$$

The matrices are in this case

$$D_R = \begin{pmatrix} x_M, y_M, r, \tau_R, 0, \frac{\pi}{2}, 0 \\ x_M, y_M, r, \tau_R, \frac{\pi}{2}, \pi - \tau_L - \tau_R, 0 \end{pmatrix}$$

$$D_L = \begin{pmatrix} -x_M, y_M, r, \tau_L, 0, \frac{\pi}{2}, 0 \\ -x_M, y_M, r, \tau_L, \frac{\pi}{2}, \pi - \tau_L - \tau_R, 0 \end{pmatrix}$$

On the following pages the results of our computations are shown for 3 examples. For each example there are one table and two illustrations. The parameters for the examples can be found in the illustrations. The values on the next table, for instance, are as follows:

For every pair y_R, y_S , the quantity γ is computed for 51 values of the angle of incidence from the range of 30° to 90° and then averaged over this range. For $y_R = -0.54, y_S = -1.7$ we find in the table $\bar{\gamma} = 0.51$. It means that in the average 51 % of the rays falling to the reflector are reflected to the collector. Therefore, for some values of κ , γ is higher, for some κ it is lower.

The variation of $\bar{\gamma}$ over the angle range is shown in the first illustration for the optimum reflector with $y_R = -0.619, y_S = -1.734$. Obviously, γ varies between 40 and 58 %. The values y_R and y_S for the optimum reflector are found as the result of a two-dimensional maximization. The method consists of 20 Monte-Carlo trials to find a rough approximation, and a gradient method to improve this value. This procedure seems lengthy, but it takes only 0,5 sec of CPU-time on an IBM 370-168. Another information to be drawn from the table is the sensitivity of γ against variation of y_S and y_R ; the sensitivity is much less with respect to y_R than with y_S .

The second illustration shows the flux per unit area. Since for the considered type of collector a "parabola effect", i.e. a large variation of the density over the area, is undesirable, this picture gives an important information. Though the third example gives the largest value of 87 % for the average γ , the corresponding reflector is useless because of the extreme variations of the density. The reflectors of the first and second example are both realistic.

$-y_S$	$-y_R$	0.09	0.18	0.27	0.36	0.45	0.54	0.63	0.72	0.81	0.90	0.99	1.08	1.17	1.26	1.35	1.44	1.53	1.62	1.71	1.80
0.00		0.23	0.24	0.25	0.26	0.27	0.27	0.28	0.29	0.29	0.30	0.30	0.30	0.29	0.27	0.25	0.23	0.20	0.17	0.14	0.11
0.10		0.22	0.23	0.24	0.25	0.26	0.27	0.28	0.28	0.29	0.29	0.30	0.29	0.28	0.27	0.24	0.22	0.19	0.16	0.14	0.12
0.20		0.22	0.23	0.23	0.24	0.25	0.26	0.27	0.28	0.28	0.29	0.29	0.29	0.28	0.26	0.24	0.21	0.18	0.17	0.15	0.13
0.30		0.21	0.22	0.23	0.24	0.25	0.26	0.26	0.27	0.28	0.28	0.28	0.28	0.27	0.25	0.23	0.21	0.19	0.18	0.16	0.14
0.40		0.21	0.22	0.22	0.23	0.24	0.25	0.26	0.26	0.27	0.27	0.27	0.27	0.26	0.25	0.23	0.22	0.20	0.19	0.17	0.15
0.50		0.21	0.21	0.22	0.23	0.24	0.24	0.25	0.26	0.26	0.27	0.27	0.27	0.27	0.26	0.24	0.23	0.21	0.20	0.18	0.16
0.60		0.21	0.22	0.23	0.23	0.24	0.25	0.26	0.27	0.27	0.28	0.28	0.28	0.28	0.26	0.25	0.24	0.22	0.21	0.19	0.17
0.70		0.22	0.22	0.23	0.24	0.25	0.26	0.27	0.27	0.28	0.29	0.29	0.29	0.29	0.27	0.26	0.25	0.23	0.22	0.20	0.18
0.80		0.22	0.23	0.24	0.25	0.25	0.26	0.27	0.28	0.29	0.29	0.30	0.30	0.29	0.28	0.27	0.25	0.24	0.22	0.21	0.19
0.90		0.23	0.24	0.25	0.25	0.26	0.27	0.28	0.29	0.30	0.30	0.31	0.31	0.30	0.29	0.27	0.26	0.25	0.24	0.22	0.21
1.00		0.24	0.25	0.26	0.27	0.28	0.28	0.29	0.30	0.31	0.31	0.32	0.32	0.31	0.30	0.29	0.27	0.26	0.25	0.24	0.23
1.10		0.26	0.26	0.27	0.28	0.29	0.30	0.31	0.32	0.32	0.33	0.34	0.33	0.32	0.31	0.30	0.29	0.28	0.28	0.27	0.26
1.20		0.28	0.29	0.29	0.30	0.31	0.32	0.33	0.34	0.34	0.35	0.36	0.35	0.34	0.33	0.32	0.32	0.31	0.31	0.31	0.31
1.30		0.31	0.31	0.32	0.33	0.34	0.35	0.36	0.37	0.37	0.38	0.38	0.37	0.37	0.36	0.36	0.35	0.35	0.35	0.35	0.35
1.40		0.34	0.35	0.36	0.37	0.38	0.39	0.39	0.40	0.41	0.42	0.41	0.41	0.40	0.40	0.39	0.39	0.39	0.39	0.38	0.39
1.50		0.39	0.40	0.41	0.41	0.42	0.43	0.44	0.45	0.45	0.45	0.45	0.44	0.43	0.43	0.42	0.42	0.42	0.42	0.41	0.41
1.60		0.43	0.44	0.45	0.46	0.47	0.47	0.48	0.48	0.48	0.48	0.47	0.46	0.46	0.45	0.45	0.45	0.44	0.44	0.44	0.43
1.70		0.47	0.48	0.49	0.50	0.50	0.51	0.51	0.51	0.50	0.49	0.49	0.48	0.47	0.47	0.46	0.46	0.45	0.45	0.44	0.44
1.80		0.46	0.47	0.48	0.48	0.49	0.49	0.49	0.48	0.48	0.47	0.47	0.46	0.46	0.45	0.45	0.45	0.44	0.43	0.43	0.43
1.90		0.40	0.40	0.41	0.41	0.41	0.41	0.41	0.40	0.40	0.40	0.40	0.40	0.40	0.39	0.39	0.39	0.38	0.38	0.38	0.38
2.00		0.22	0.22	0.23	0.23	0.24	0.24	0.25	0.25	0.26	0.26	0.27	0.27	0.28	0.28	0.29	0.29	0.30	0.31	0.31	0.32

48

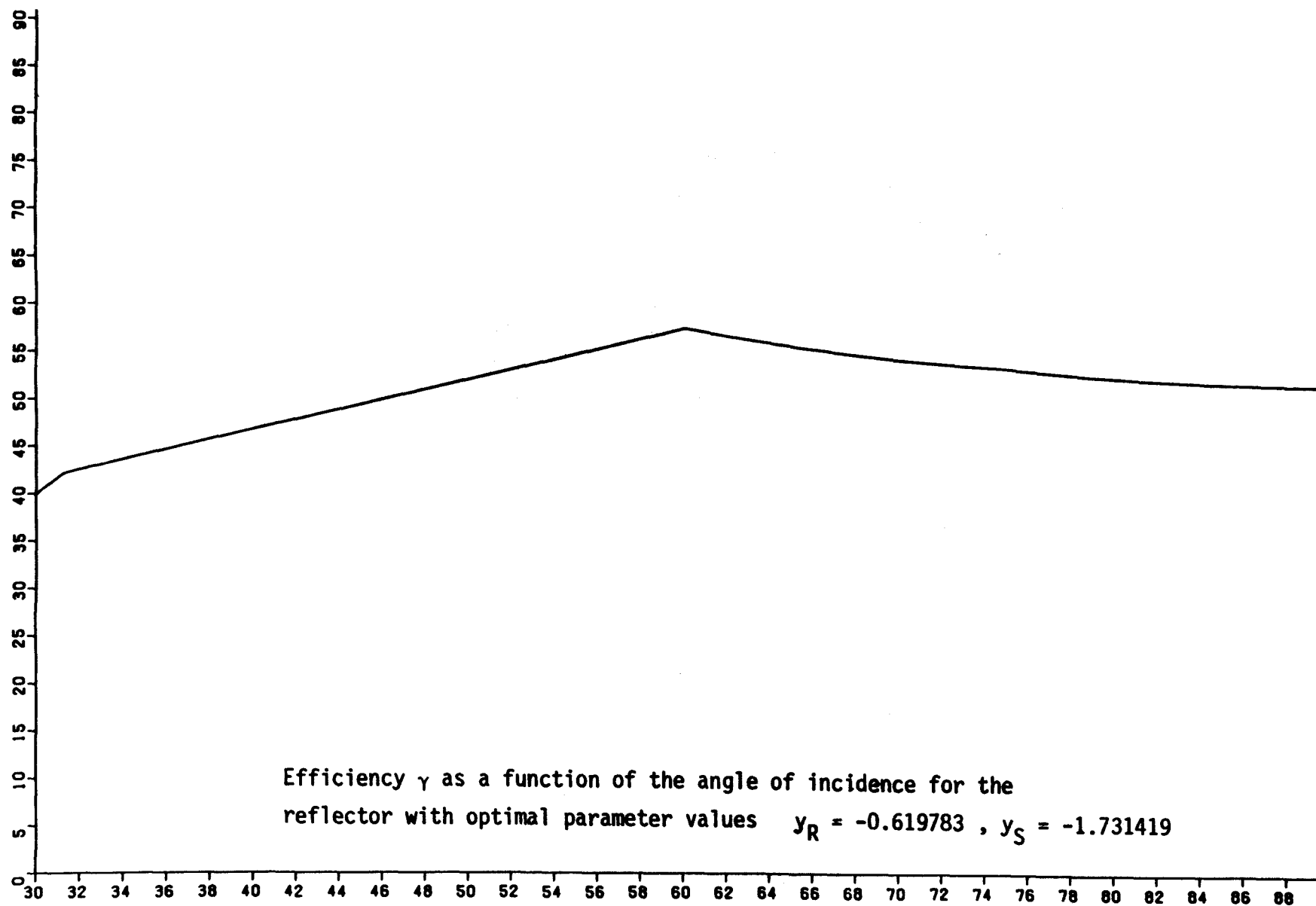
Efficiency γ , averaged over the angle range $30^\circ - 90^\circ$, as a function of y_R and y_S ($x_R=3$, $d=+2$).

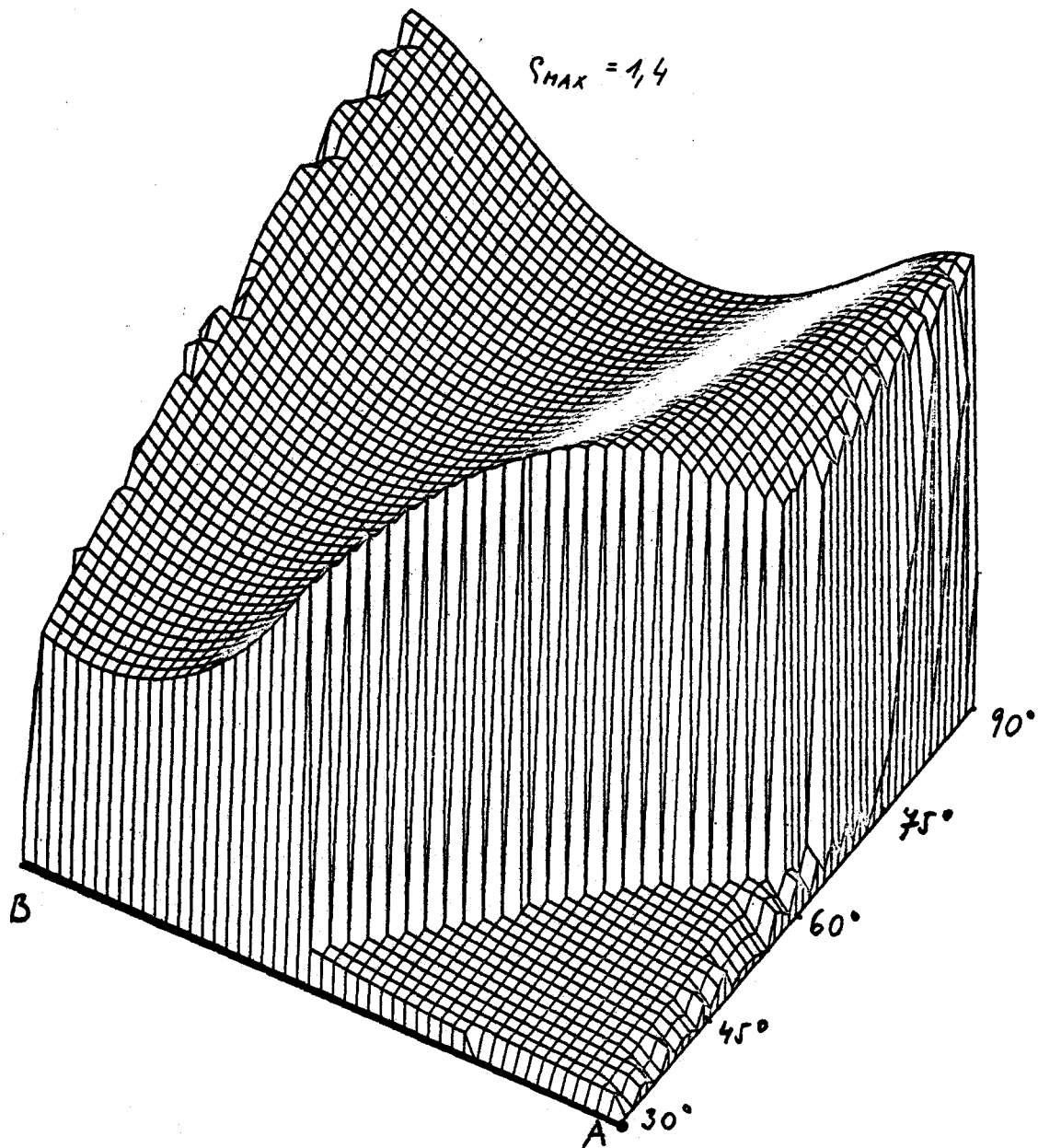
The maximum efficiency occurs for $y_R = -0.619783$ $y_S = -1.731419$

Center = (1.027, 0.100)

Radius = 2.100

Maximum = 0.515394





Flux per unit area on the collector as a function of the angle of incidence for the reflector with optimal parameter values $y_R = -0.619783$, $y_S = -1.731419$

$-y_s$	$-y_R$	0.09	0.18	0.27	0.36	0.45	0.54	0.63	0.72	0.81	0.90	0.99	1.08	1.17	1.26	1.35	1.44	1.53	1.62	1.71	1.80
0.00	0.26	0.26	0.27	0.27	0.27	0.27	0.27	0.27	0.26	0.26	0.26	0.26	0.26	0.25	0.25	0.24	0.23	0.20	0.16	0.11	0.07
0.10	0.26	0.26	0.26	0.26	0.26	0.26	0.26	0.26	0.26	0.26	0.26	0.26	0.25	0.25	0.25	0.24	0.22	0.19	0.15	0.11	0.08
0.20	0.26	0.26	0.26	0.26	0.26	0.26	0.26	0.26	0.26	0.26	0.25	0.25	0.25	0.25	0.24	0.23	0.21	0.18	0.15	0.12	0.08
0.30	0.25	0.25	0.25	0.25	0.25	0.25	0.25	0.25	0.25	0.25	0.25	0.25	0.25	0.24	0.23	0.22	0.21	0.19	0.16	0.13	0.09
0.40	0.25	0.25	0.25	0.25	0.25	0.25	0.25	0.25	0.25	0.25	0.25	0.24	0.24	0.23	0.23	0.23	0.22	0.20	0.17	0.13	0.09
0.50	0.24	0.24	0.24	0.24	0.24	0.24	0.24	0.24	0.24	0.24	0.24	0.24	0.24	0.24	0.24	0.24	0.23	0.21	0.18	0.14	0.10
0.60	0.25	0.25	0.25	0.25	0.25	0.25	0.25	0.25	0.25	0.25	0.25	0.25	0.25	0.25	0.25	0.24	0.24	0.22	0.18	0.14	0.10
0.70	0.25	0.25	0.25	0.25	0.25	0.25	0.25	0.25	0.25	0.25	0.25	0.25	0.25	0.25	0.25	0.25	0.24	0.22	0.18	0.14	0.10
0.80	0.26	0.26	0.26	0.26	0.26	0.26	0.26	0.26	0.26	0.26	0.26	0.26	0.26	0.26	0.26	0.26	0.25	0.25	0.22	0.19	0.15
0.90	0.26	0.26	0.26	0.26	0.26	0.26	0.26	0.26	0.26	0.26	0.26	0.26	0.26	0.26	0.26	0.26	0.25	0.23	0.19	0.15	0.10
1.00	0.27	0.27	0.27	0.27	0.27	0.27	0.27	0.27	0.27	0.27	0.27	0.27	0.27	0.27	0.27	0.27	0.26	0.23	0.20	0.15	0.10
1.10	0.28	0.28	0.28	0.28	0.28	0.28	0.28	0.28	0.28	0.28	0.28	0.28	0.28	0.28	0.28	0.28	0.27	0.24	0.20	0.16	0.11
1.20	0.30	0.30	0.30	0.30	0.30	0.30	0.30	0.30	0.30	0.30	0.30	0.30	0.30	0.30	0.30	0.30	0.28	0.25	0.21	0.17	0.11
1.30	0.32	0.31	0.31	0.31	0.31	0.31	0.31	0.32	0.32	0.32	0.32	0.32	0.32	0.32	0.32	0.32	0.32	0.30	0.26	0.23	0.18
1.40	0.34	0.34	0.34	0.34	0.34	0.34	0.34	0.34	0.34	0.34	0.35	0.35	0.35	0.35	0.35	0.34	0.32	0.29	0.25	0.20	0.13
1.50	0.37	0.37	0.37	0.37	0.37	0.38	0.38	0.38	0.38	0.38	0.38	0.39	0.39	0.39	0.40	0.38	0.35	0.32	0.28	0.24	0.18
1.60	0.42	0.42	0.42	0.42	0.42	0.43	0.43	0.43	0.44	0.44	0.45	0.45	0.46	0.46	0.44	0.42	0.39	0.36	0.32	0.26	
1.70	0.49	0.49	0.49	0.50	0.50	0.50	0.51	0.51	0.52	0.53	0.54	0.55	0.55	0.54	0.52	0.49	0.46	0.43	0.38	0.31	
1.80	0.50	0.50	0.51	0.52	0.53	0.54	0.55	0.57	0.58	0.59	0.61	0.61	0.61	0.59	0.57	0.54	0.51	0.48	0.43	0.35	
1.90	0.45	0.46	0.47	0.48	0.50	0.52	0.55	0.57	0.60	0.62	0.63	0.62	0.61	0.60	0.59	0.57	0.54	0.51	0.45	0.38	
2.00	0.33	0.35	0.39	0.43	0.47	0.48	0.49	0.50	0.51	0.52	0.53	0.54	0.56	0.58	0.58	0.56	0.51	0.46	0.41	0.36	

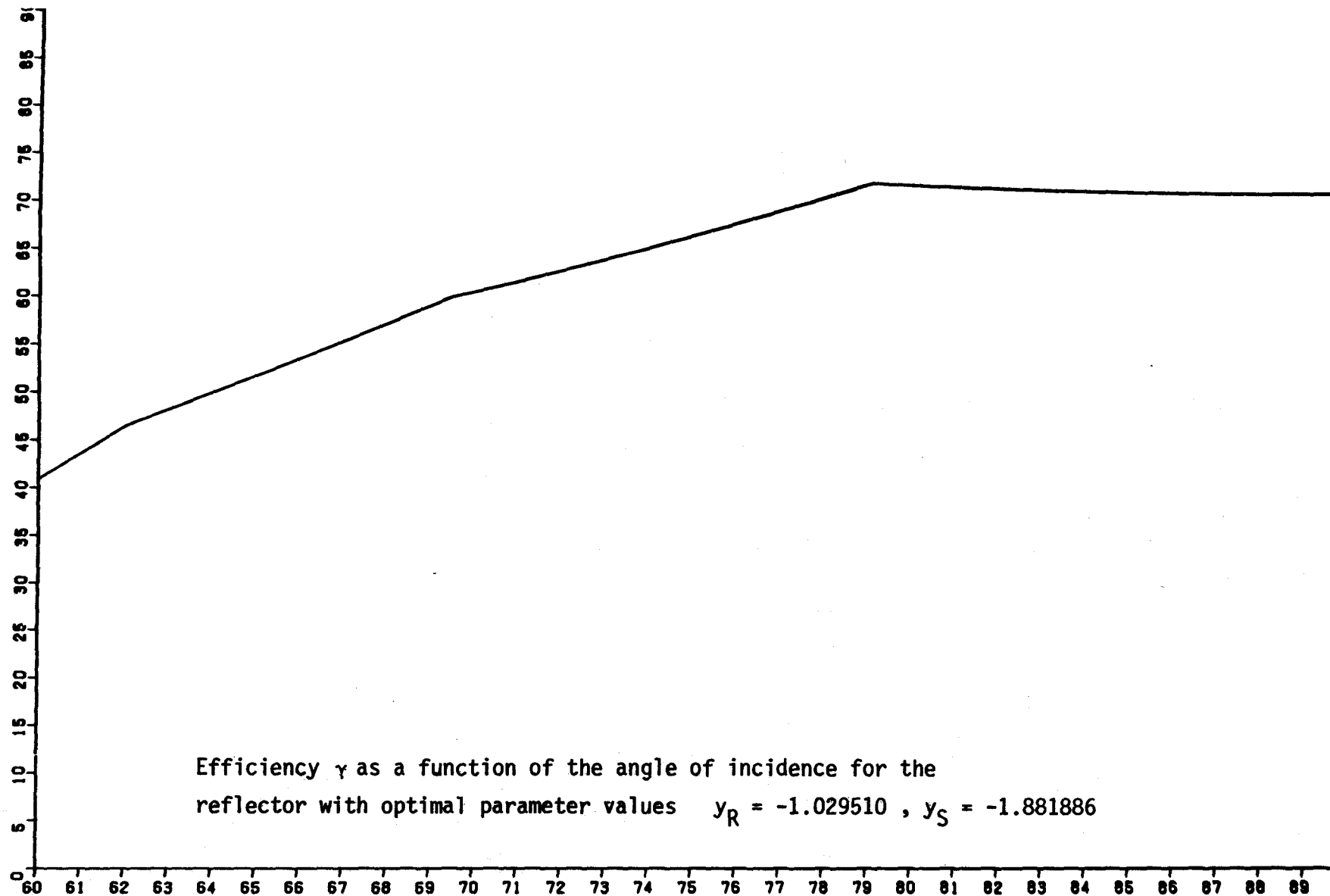
Efficiency γ , averaged over the angle range $60^\circ - 90^\circ$, as a function of y_R and y_S ($x_R=3$, $d=-2$)

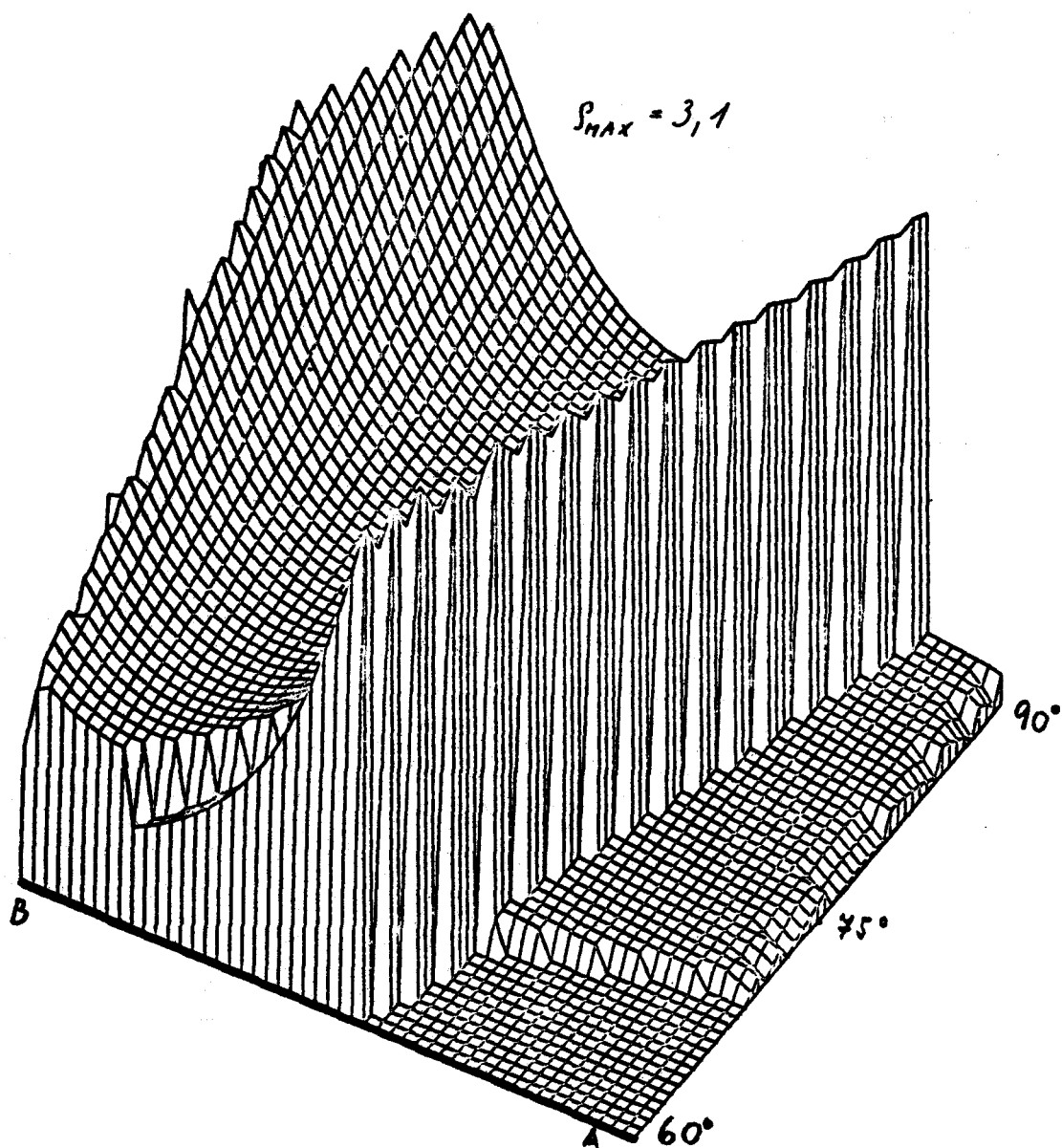
The maximum efficiency occurs for $y_R = -1.029510$ $y_S = -1.881886$

Center = (0.823, 0.927)

Radius = 2.927

Maximum = 0.629171





Flux per unit area on the collector as a function of the angle of incidence for the reflector with optimal parameter values $y_R = -1.029510$, $y_S = -1.881886$

$-y_s$	$-y_R$	0.09	0.18	0.27	0.36	0.45	0.54	0.63	0.72	0.81	0.90	0.99	1.08	1.17	1.26	1.35	1.44	1.53	1.62	1.71	1.80	
0.00		0.25	0.26	0.26	0.26	0.26	0.26	0.26	0.26	0.25	0.25	0.25	0.25	0.25	0.24	0.24	0.23	0.21	0.18	0.12	0.06	
0.10		0.25	0.25	0.25	0.25	0.25	0.25	0.25	0.25	0.25	0.25	0.25	0.25	0.24	0.24	0.23	0.22	0.20	0.17	0.12	0.06	
0.20		0.25	0.25	0.25	0.25	0.25	0.25	0.25	0.25	0.25	0.25	0.24	0.24	0.24	0.24	0.23	0.21	0.19	0.17	0.13	0.06	
0.30		0.24	0.25	0.25	0.25	0.25	0.25	0.25	0.25	0.25	0.24	0.24	0.24	0.23	0.23	0.21	0.20	0.20	0.18	0.13	0.06	
0.40		0.24	0.24	0.24	0.24	0.24	0.24	0.24	0.24	0.24	0.24	0.24	0.23	0.22	0.22	0.22	0.22	0.21	0.20	0.14	0.06	
0.50		0.24	0.24	0.24	0.24	0.24	0.24	0.24	0.24	0.24	0.24	0.24	0.24	0.23	0.23	0.23	0.23	0.22	0.20	0.14	0.06	
0.60		0.24	0.24	0.24	0.24	0.24	0.24	0.24	0.24	0.24	0.24	0.24	0.24	0.24	0.24	0.24	0.23	0.23	0.20	0.14	0.06	
0.70		0.25	0.25	0.25	0.25	0.25	0.25	0.25	0.25	0.25	0.25	0.25	0.24	0.24	0.24	0.24	0.24	0.23	0.21	0.14	0.06	
0.80		0.25	0.25	0.25	0.25	0.25	0.25	0.25	0.25	0.25	0.25	0.25	0.25	0.25	0.25	0.24	0.24	0.24	0.21	0.14	0.05	
0.90		0.26	0.26	0.26	0.26	0.26	0.26	0.26	0.26	0.26	0.26	0.26	0.25	0.25	0.25	0.25	0.25	0.24	0.21	0.14	0.05	
1.00		0.26	0.26	0.26	0.26	0.26	0.26	0.26	0.26	0.26	0.26	0.26	0.26	0.26	0.26	0.26	0.26	0.25	0.21	0.14	0.05	
1.10		0.27	0.27	0.27	0.27	0.27	0.27	0.27	0.27	0.27	0.27	0.27	0.27	0.27	0.27	0.27	0.27	0.26	0.22	0.13	0.04	
1.20		0.29	0.29	0.29	0.29	0.29	0.29	0.29	0.29	0.29	0.29	0.29	0.29	0.29	0.29	0.29	0.29	0.28	0.27	0.22	0.13	0.04
1.30		0.30	0.30	0.30	0.30	0.30	0.30	0.30	0.31	0.31	0.31	0.31	0.31	0.31	0.31	0.31	0.31	0.30	0.28	0.22	0.13	0.03
1.40		0.33	0.33	0.33	0.33	0.33	0.33	0.33	0.33	0.33	0.33	0.33	0.34	0.34	0.34	0.34	0.34	0.33	0.30	0.22	0.12	0.03
1.50		0.36	0.36	0.36	0.36	0.36	0.36	0.36	0.37	0.37	0.37	0.37	0.37	0.37	0.38	0.38	0.38	0.37	0.32	0.22	0.11	0.02
1.60		0.41	0.41	0.41	0.41	0.41	0.41	0.41	0.42	0.42	0.42	0.43	0.43	0.44	0.44	0.44	0.44	0.41	0.34	0.23	0.10	0.01
1.70		0.48	0.48	0.48	0.48	0.48	0.49	0.49	0.50	0.50	0.51	0.52	0.53	0.54	0.54	0.53	0.49	0.39	0.26	0.10	0.01	
1.80		0.48	0.48	0.49	0.50	0.51	0.53	0.54	0.56	0.59	0.61	0.63	0.65	0.67	0.69	0.66	0.59	0.48	0.33	0.18	0.07	
1.90		0.43	0.44	0.45	0.47	0.48	0.50	0.53	0.56	0.60	0.64	0.70	0.75	0.79	0.78	0.72	0.63	0.50	0.37	0.23	0.15	
2.00		0.32	0.35	0.39	0.43	0.48	0.53	0.60	0.68	0.76	0.84	0.85	0.83	0.78	0.69	0.59	0.49	0.39	0.31	0.25	0.20	

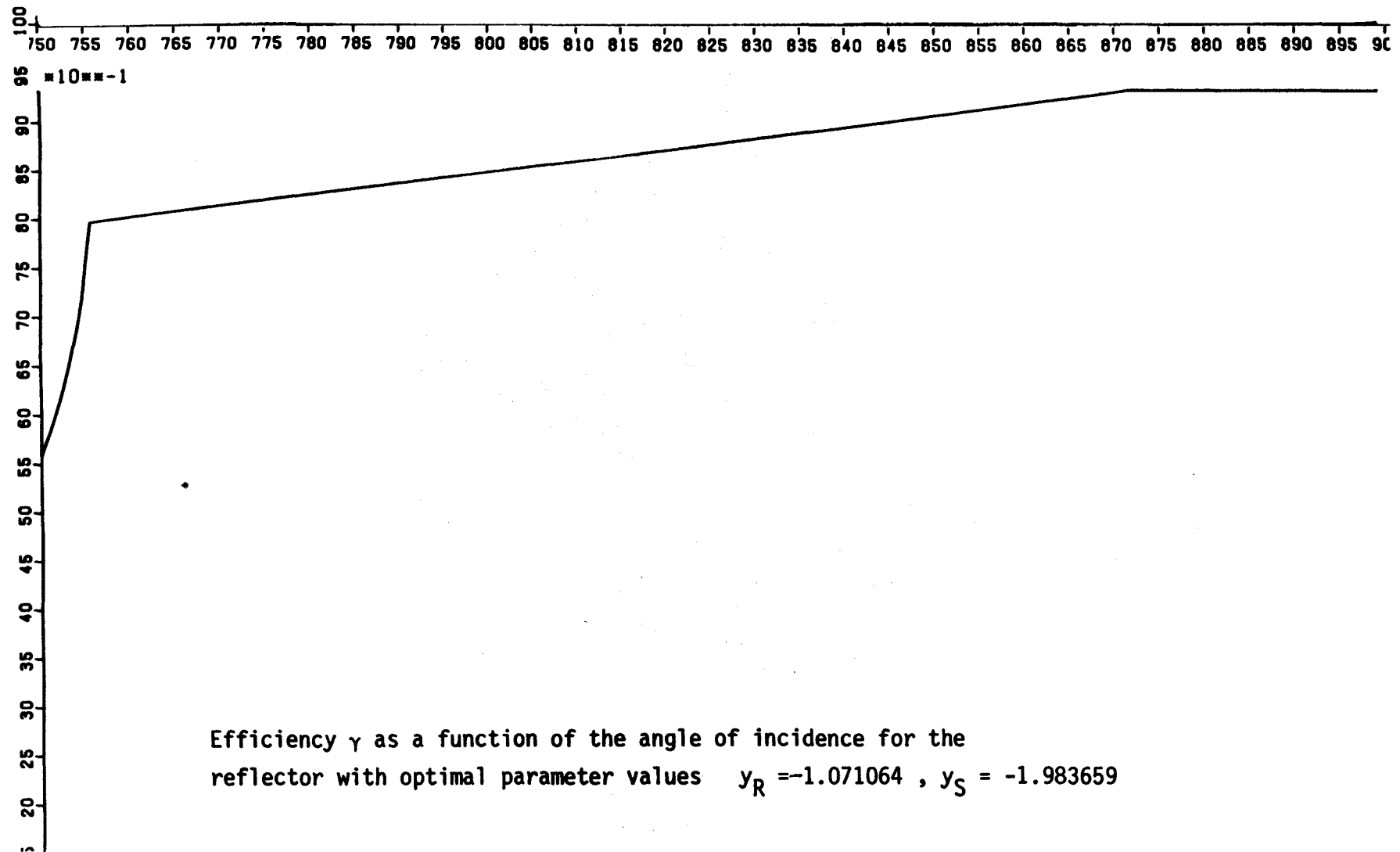
Efficiency γ , averaged over the angle range $75^\circ - 90^\circ$, as a function of y_R and y_S ($x_R=3$, $d=-2$).

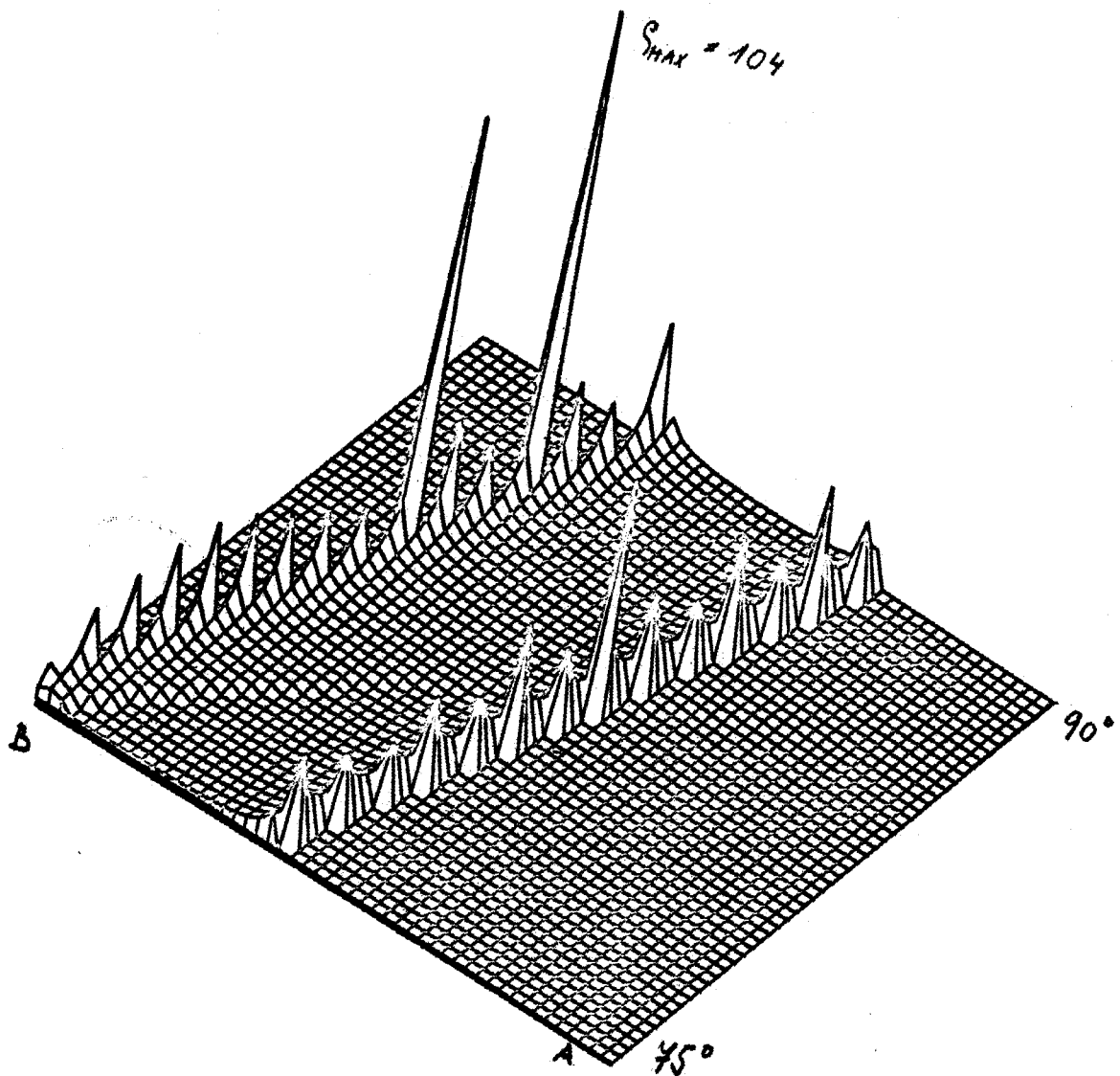
The maximum efficiency occurs for $y_R = -1.071064$ $y_S = -1.983659$

Center = (0.370, 2.189)

Radius = 4.189

Maximum = 0.866780





Flux per unit area on the collector as a function of the angle of incidence for the reflector with optimal parameter values
 $y_R = -1.071064$, $y_S = -1.983659$

Literature

- /1/ A.F. Souka, "Double Exposure Flat Plate Collector",
Solar Energy, 9, 3, (1965), p. 117.

- /2/ A.F. Souka, H.H. Safwal, "Optimum Orientations for the Double-
Exposure, Flat Plate Collector and its Reflectors",
Solar Energy, Phoenix, Ariz., Vol. 10, (1966), pp 170-174.

- /3/ G. Falbel, "The FES Delta Focusing Solar Collector",
SPIE Vol. 68 (1975), Solar Energy Utilization.

- /4/ F. Kreith, J.F. Kreider, "Principles of Solar Engineering",
New York 1978.

- /5/ A.B. Meinel, M.P. Meinel, "Applied Solar Energy",
Reading, Mass. 1976.